An endogenous chemorepellent directs cell movement by inhibiting pseudopods at one side of cells

Ramesh Rijal, Kristen M. Consalvo, Christopher K. Lindsey, and Richard H. Gomer*
Department of Biology, Texas A&M University, College Station, TX 77843-3474

ABSTRACT **Eukaryotic chemoattraction signal transduction pathways, such as those used by *Dictyostelium discoideum* to move toward cAMP, use a G protein–coupled receptor to activate multiple conserved pathways such as PI3 kinase/Akt/PKB to induce actin polymerization and pseudopod formation at the front of a cell, and PTEN to localize myosin II to the rear of a cell. Relatively little is known about chemorepulsion. We previously found that AprA is a chemorepellent protein secreted by *Dictyostelium* cells. Here we used 29 cell lines with disruptions of cAMP and/or AprA signal transduction pathway components, and delineated the AprA chemorepulsion pathway. We find that AprA uses a subset of chemoattraction signal transduction pathways including Ras, protein kinase A, target of rapamycin (TOR), phospholipase A, and ERK1, but does not require the PI3 kinase/Akt/PKB and guanylyl cyclase pathways to induce chemorepulsion. Possibly as a result of not using the PI3 kinase/Akt/PKB pathway and guanylyl cyclases, AprA does not induce actin polymerization or increase the pseudopod formation rate, but rather appears to inhibit pseudopod formation at the side of cells closest to the source of AprA.**

Monitoring Editor
Carole Parent
University of Michigan

Received: Sep 7, 2018
Revised: Nov 7, 2018
Accepted: Nov 14, 2018

INTRODUCTION

Directed movement of eukaryotic cells by chemoattraction or chemorepulsion is critical during embryogenesis (Theveneau and Mayor, 2012), the trafficking of immune cells during inflammation (Sadik and Luster, 2012; Kolaczkowska and Kubes, 2013), and parasite pathogenicity (Zaki *et al.*, 2006). Although a considerable amount is known about the mechanisms of chemoattraction, relatively little is known about chemorepulsion. Studies on the movement of starved *Dictyostelium discoideum* cells toward cyclic adenosine monophosphate (cAMP) and folate have elucidated chemoattraction signal transduction pathways (Chen *et al.*, 2007; Kortholt *et al.*, 2011). In a cAMP gradient, *Dictyostelium* cells use a G protein–coupled cAMP receptor to induce F-actin–driven pseudopods and filopods to move toward the cAMP (Klein *et al.*, 1988; Kumagai *et al.*, 1989; Nichols *et al.*, 2015). Rather than a single pathway, at least six different signal transduction pathways act downstream from the cAMP receptor to mediate motility. These pathways include PI3K/PIP3, TorC2, phospholipase A, guanylyl cyclase, MAPK, and ElmoE (Ma *et al.*, 1997; Kortholt *et al.*, 2011; Yan *et al.*, 2012). For chemotaxis toward folate, *Dictyostelium* cells use a folate receptor, the G proteins Gα4, Gβ, and Gγ, and Ras (De Wit and Bulgakov, 1985; Hadwiger *et al.*, 1994; Lim *et al.*, 2005). Unlike chemoattraction to cAMP, cells moving toward folate do not require

This article was published online ahead of print in MBoC in Press (http://www.molbiolcell.org/cgi/doi/10.1091/mbc.E18-09-0562) on November 21, 2018.

Author contributions: R.R. designed, performed, and analyzed experiments and wrote the paper. K.M.C. performed and analyzed experiments and wrote the paper. C.L. performed and analyzed experiments. R.H.G. designed experiments and wrote the paper.

*Address correspondence to: Richard H. Gomer (rgomer@tamu.edu).

Abbreviations used: ANOVA, analysis of variance; cAMP, cyclic adenine monophosphate; CRAC, cytosolic regulator of adenylyl cyclase; DAPI, 4′,6-diamidino-2-phenylindole; DIC, differential interference contrast; DPPIV, dipeptidyl peptidase IV; ECL, enhanced chemiluminescence; EGTA, ethylene glycol tetraacetic acid; ElmoE, engulfment and cell motility E; ERK, extracellular signal-regulated kinase; F-actin, filamentous actin; FMI, forward migration index; GFP, green fluorescent protein; InsP_3Rs, inositol triphosphate receptors; MAPK, mitogen-activated kinases; MHC II, myosin II heavy chain; NF1, neurofibromin; PakD, p21-activated kinase; PBS, phosphate-buffered saline; PI3K, phosphoinositide-3-kinase; PIP2, phosphatidylinositol (4,5)-bisphosphate; PIP3, phosphatidylinositol (3,4,5)-trisphosphate; PIPES, piperazine-*N*,*N*′-bis(2-ethanesulfonic acid); PlaA, phospholipase A; PTEN, phosphatase and tensin homologue; rAprA, recombinant AprA; RBD, Ras-binding domain; RT-PCR, reverse transcription PCR; SCAR, suppressor of cAR; TAME, *N*-α-*p*-tosyl-L-arginine methyl ester hydrochloride; TOR, target of rapamycin; TORC1, target of rapamycin complex 1; WASP, Wiskott–Aldrich syndrome protein; WT, wild type.

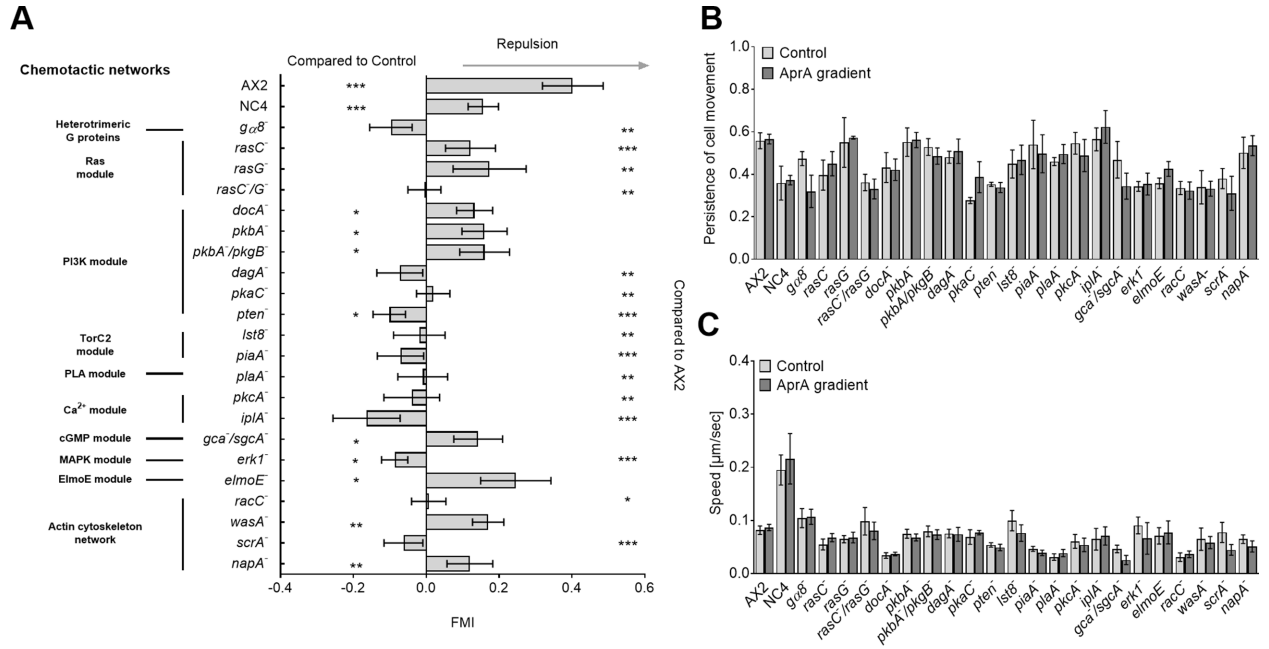

FIGURE 1: AprA uses some but not all components of the cAMP signal transduction pathways. (A) Cells of the indicated strains were imaged for 40 min in growth medium (control) or in an AprA gradient in growth medium in Insall chambers. A positive forward migration index (FMI) indicates chemorepulsion from the AprA and a negative FMI indicates chemoattraction. Values are mean ± SEM from at least 30 cells per strain from ≥3 independent experiments. At left, * indicates $p < 0.05$, ** indicates $p < 0.01$, and *** indicates $p < 0.001$ compared with control for that genotype (*t* tests). At right, * indicates $p < 0.05$, ** indicates $p < 0.01$, and *** indicates $p < 0.001$ compared with wild-type (WT; *t* tests). (B, C) The data analyzed for A were also analyzed for persistence of cell movement and cell speed.

PI3K, TorC2, phospholipase A, or guanylyl cyclase signal transduction pathways (Kortholt *et al.*, 2011).

By activating the cAMP receptor in a different way compared with cAMP, a synthetic analogue of cAMP acts as a chemorepellent by activating the G protein Gα1 and inhibiting phospholipase C to cause an accumulation of PI(3,4,5)P3 at the side of the cell farthest from the source of the analogue of cAMP, and myosin contraction at the side of the cell closest to the source of the analogue of cAMP, which results in the cell moving away from the source of the cAMP analogue (Van Haastert *et al.*, 1984; Keizer-Gunnink *et al.*, 2007; Cramer *et al.*, 2018). AprA is an endogenous secreted protein that induces chemorepulsion of *Dictyostelium* cells (Phillips and Gomer, 2012). An orthologue of AprA, dipeptidyl peptidase IV (DPPIV), acts as a chemorepellent for neutrophils (Herlihy *et al.*, 2013a, 2015, 2017; White *et al.*, 2018). Unlike the repetitive pulses of cAMP that drive *Dictyostelium* aggregation during development, AprA appears to be continuously secreted by growing cells, and appears to help cells at the edge of a colony to move away from the colony to find new sources of food. Compared to cAMP pulses, endogenous AprA gradients thus have a negligible temporal component. Cells sense AprA using the G-protein–coupled receptor GrlH to induce chemorepulsion (Tang *et al.*, 2018). Although loss of phospholipase C or PI3 kinases 1 and 2 reduce chemoattraction to cAMP, cells lacking these components still move away from AprA (Phillips and Gomer, 2012). In this article, we show that in addition to not needing phospholipase C or PI3 kinases 1 and 2, AprA chemorepulsion also does not require the cAMP chemoattraction components protein kinase B, guanylyl cyclase, ElmoE, WasA, and NapA, and that AprA prevents pseudopod formation at the side of a cell closest to the source of AprA, resulting in a movement away from AprA.

RESULTS

AprA chemorepulsion uses a G-protein–coupled receptor, G proteins, and Ras

In cAMP-mediated chemoattraction, several pathways act downstream from the cAMP receptor (Kortholt *et al.*, 2011; Yan *et al.*, 2012). To compare the pathway(s) mediating AprA chemorepulsion to the cAMP chemoattraction pathways, we used an Insall chamber to determine whether AprA could induce chemorepulsion in cells lacking key components of the different pathways. A calculation of the theoretical amount of AprA at various distances from the center of a colony of cells indicated that a 0–300 ng/ml AprA gradient in the Insall chamber would reasonably approximate the natural AprA gradient at the edge of the colony (Supplemental Figure S1), and this gradient was used for the work in this article. The movement of cells toward or away from the AprA source in the Insall chamber was measured as the forward migration index (FMI), with a positive FMI indicating chemorepulsion. Defining the *x*-axis as being parallel to the gradient, FMI is the *x*-axis distance component of a cell's movement over the course of the experiment divided by the integrated distance the cell moved along its path. As previously observed, AprA caused chemorepulsion of wild-type AX2 cells (Figure 1A; Phillips and Gomer, 2012). In addition, AprA caused chemorepulsion of wild-type NC4, and chemorepulsion of the axenic strains AX3, AX4, KAX3, JH8, and JH10 (Supplemental Figure S2A). The axenic strains (AX2, AX3, AX4, KAX3, JH8, and JH10) have a mutation in the *axeB* gene encoding neurofibromin (NF1), which causes them to have increased macropinocytosis compared with the nonaxenic NC4 cells (Veltman *et al.*, 2014; Bloomfield *et al.*, 2015). Unlike the axenic strains, NC4 cells were grown on bacteria, so axenic and nonaxenic cells, and cells grown in axenic media and on bacteria, responded to AprA.

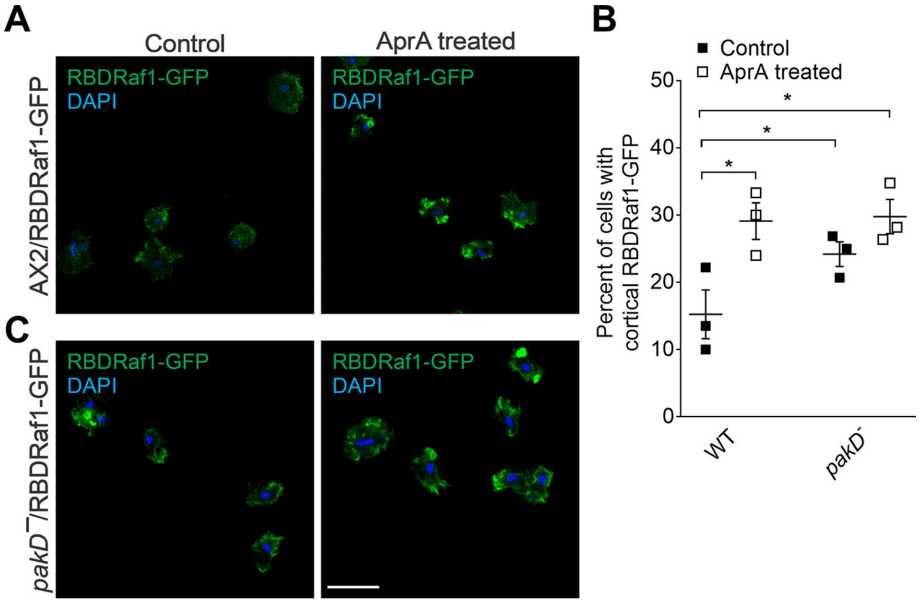

FIGURE 2: AprA causes activation of Ras. (A–C) Localization of the Ras-binding protein RBDRaf1-GFP in wild-type AX2 and *pakD*⁻ cells incubated with a uniform concentration of AprA or buffer (control) for 20 min, fixed and stained with DAPI (blue); bar is 20 μm. (B) Quantification of RBDRaf1-GFP translocation in cells. Images are representative of, and data are mean ± SEM of three independent experiments. * indicates $p < 0.05$ (two-way ANOVA; Fisher's LSD test).

The cAMP pathway requires the G-protein–coupled receptor cAR1 and the G proteins Gα2 and Gβ (Wu *et al.*, 1995; Parent and Devreotes, 1996). We previously observed that AprA binds to the G-protein–coupled receptor GrlH, requires GrlH and the G protein Gβ to inhibit proliferation and to induce chemorepulsion, and uses the G protein Gα8 to inhibit proliferation (Bakthavatsalam *et al.*, 2009; Phillips and Gomer, 2012; Tang *et al.*, 2018). We observed that compared with wild type, *gα8*⁻ cells did not move away from AprA (Figure 1A). Although these cells appeared to move toward AprA, the effect was not statistically significant. Cells lacking either of the Ras proteins RasC or RasG show chemoattraction to cAMP, whereas cells lacking both RasC and RasG move randomly in cAMP gradients (Kortholt *et al.*, 2011). Although *rasC*⁻ and *rasG*⁻ cells moved away from AprA, *rasC*⁻/*rasG*⁻ cells did not (Figure 1A). Ras activation can be assessed by examining the translocation to the cell cortex of a chimeric protein containing the Ras-binding domain (RBD) of the serine/threonine kinase Raf1 and green fluorescent protein (GFP; Kortholt and van Haastert, 2008), and cAMP induces this translocation (Kortholt and van Haastert, 2008). Compared to buffer treated wild-type cells, AprA also induced the translocation of RBDRaf1-GFP to the cell cortex (Figure 2, A and B). In addition, using a pull-down assay of active Ras with Raf-RBD affinity beads, we observed that compared with buffer treated wild-type cells, AprA activated Ras within 5 min (Supplemental Figure S3, A and B). The anti-Ras antibodies appeared to detect multiple bands, and these may be some of the 11 different Ras gene products in *Dictyostelium* (Kortholt and van Haastert, 2008). We did not observe RBDRaf1-GFP concentrated at the cortex in *grlH*⁻ cells, suggesting that RBDRaf1-GFP translocation to the membrane in vegetative cells requires GrlH (Supplemental Figure S4A). Together, these results indicate that cAMP and AprA chemotaxis both use G protein–coupled receptors, G proteins, and Ras, and that both involve receptor-mediated activation of Ras.

AprA chemorepulsion does not need, nor appear to activate, PI3 kinase pathway components such as Akt

Downstream from G proteins and Ras, PI3 kinase is part of one pathway that potentiates, but is not required for, cAMP chemoattraction (Andrew and Insall, 2007). We previously observed that PI3 kinases 1 and 2 are not required for AprA chemorepulsion (Phillips and Gomer, 2012). Other components of the PI3 kinase pathway include the Dock180-related RacGEF DockA, the Akt/PKB protein kinase PkbA, the SGK family protein kinase PkgB, the *dagA* product CRAC (cytosolic regulator of adenylyl cyclase, a pleckstrin homology [PH] domain–containing protein), and the cAMP-dependent protein kinase A catalytic subunit PkaC. Loss or mutation of these proteins causes partial defects in cAMP chemotaxis (Meili *et al.*, 2000; Comer *et al.*, 2005; Para *et al.*, 2009; Scavello *et al.*, 2017). Phosphatase and tensin homologue (PTEN) regulates PI3 kinase signaling by dephosphorylating the PI3 kinase product PI(3,4,5)P3 to PI(4,5)P2 (Maehama and Dixon, 1998). Loss of PTEN partially decreases chemotaxis to cAMP (Iijima and Devreotes, 2002). *docA*⁻, *pkbA*⁻, and *pkbA*⁻/*pkgB*⁻ cells moved away from AprA, while *dagA*⁻, *pkaC*⁻, and *pten*⁻ cells did not (Figure 1A), indicating that some but not all components of the PI3 kinase pathway are necessary for AprA chemorepulsion, and that some PI3 kinase pathway proteins that help cAMP chemoattraction are not needed for AprA chemorepulsion.

cAMP-induced activation of PI3K causes activation of the kinase Akt/PKB, which results in cAMP-induced phosphorylation at Akt substrate sites of many proteins (Cai *et al.*, 2010). To determine whether AprA has a similar, and possible long-term, effect on Akt substrate phosphorylation, we incubated wild-type cells with AprA, and stained cells and Western blots of cell lysates for phosphorylated Akt substrates. Although AprA appeared to slightly increase levels of the phosphorylated form of a ~19 kDa Akt substrate, the effect was not statistically significant, and although AprA gradients appeared to slightly increase levels of phosphorylated Akt substrates at the side of the cell away from the source of the AprA, this effect also was not statistically significant (Supplemental Figure S5, A–D). These results suggest that AprA does not significantly activate Akt.

AprA chemorepulsion uses TORC2, phospholipase A, a Ca^{2+} channel, and protein kinase C

The target of rapamycin (TOR) is a protein complex that exists in two functionally different forms, TOR complex 1 (TORC1) and TORC2 (Zoncu *et al.*, 2011). TORC2 is a major regulator of the actin cytoskeleton (Schmidt *et al.*, 1996). The TORC2 components Lst8 and PiaA mediate cAMP chemoattraction downstream from G proteins and Ras, and loss of Lst8 or PiaA leads to a partial inhibition of chemotaxis in cAMP gradients (Lee *et al.*, 2005). *lst8*⁻ and *piaA*⁻ cells did not move away from AprA (Figure 1A), suggesting that whereas TORC2 facilitates cAMP chemoattraction, TORC2 is necessary for AprA chemorepulsion.

Phospholipase A is part of another pathway that mediates cAMP chemoattraction downstream from G proteins and Ras (Chen *et al.*, 2007), and loss of phospholipase A (PlaA) causes cells to have

reduced persistence of movement toward cAMP (Bosgraaf and Van Haastert, 2009). *plaA*$^-$ cells did not move away from AprA (Figure 1A), suggesting that phospholipase A is necessary for AprA chemorepulsion.

cAMP causes a rise in intracellular Ca^{2+} levels by inducing Ca^{2+} influx (Traynor *et al.*, 2000). The plasma membrane Ca^{2+} channel IplA is homologous to the inositol trisphosphate receptors ($InsP_3Rs$) of higher eukaryotes (Traynor *et al.*, 2000). Disruption of *iplA* in *Dictyostelium* blocks cAMP-stimulated Ca^{2+} influx, but does not appear to affect chemoattraction toward cAMP (Lusche *et al.*, 2012). *iplA*$^-$ cells did not move away from AprA (Figure 1A). The protein kinase C orthologue PkcA is involved in both Ca^{2+}-dependent and -independent signaling during cAMP chemotaxis, and *pkcA*$^-$ cells show chemotaxis toward cAMP but with an abnormally high cell speed (Mohamed *et al.*, 2015). *pkcA*$^-$ cells did not move away from AprA (Figure 1A). These results suggest that IplA and PkcA, although not necessary for chemoattraction toward cAMP, are necessary for chemorepulsion from AprA.

AprA chemorepulsion does not require guanylyl cyclases

In addition to the PI3 kinase pathway, the TorC2 pathway, and the phospholipase A pathway, guanylyl cyclases mediate cAMP chemoattraction downstream from G proteins and Ras (Bolourani *et al.*, 2006). *Dictyostelium* has two guanylyl cyclases: the membrane-bound guanylyl cyclase GcA and the soluble guanylyl cyclase SgcA (Roelofs and Van Haastert, 2002). cAMP stimulates the activation of guanylyl cyclase in wild-type cells (van Haastert and Kuwayama, 1997). *gca*$^-$*/sgcA*$^-$ cells, lacking both guanylyl cyclases, show defects in chemotaxis toward cAMP (Roelofs and Van Haastert, 2002). However, *gca*$^-$*/sgcA*$^-$ cells moved away from AprA (Figure 1A), suggesting that guanylyl cyclases are not necessary for AprA chemorepulsion.

AprA chemorepulsion requires the MAPK ERK1

Extracellular signal–regulated kinases (ERKs) are a conserved group of mitogen-activated kinases (MAPKs; Cargnello and Roux, 2011). *Dictyostelium* has two MAPKs, ERK1 and ERK2 (Hadwiger and Nguyen, 2011). In starved cells, cAMP causes a rapid increase in ERK2 phosphorylation, which is followed by an increase in ERK1 phosphorylation, and the ERK1 phosphorylation can be detected by an anti-phospho MAPK antibody that detects threonine phosphorylation at a conserved TXY motif (Schwebs and Hadwiger, 2015). Loss of ERK1 causes strong defects in directionality and speed of the cells toward cAMP (Sobko *et al.*, 2002). *erk1*$^-$ cells did not move away from AprA (Figure 1A), and actually appeared to move toward AprA. However, AprA did not significantly affect the levels of ERK1 phosphorylation at the conserved TXY motif (Supplemental Figure S6A), suggesting that ERK1, but not ERK1 phosphorylation at the TXY motif, is necessary for AprA chemorepulsion.

AprA chemorepulsion requires RacC and SCAR

Movement of cells toward cAMP involves regulation of the actin cytoskeleton (Devreotes and Horwitz, 2015). A Gβγ effector, ElmoE (engulfment and cell motility E), links cAMP receptor signaling to the actin cytoskeleton during chemotaxis, and *elmoE*$^-$ cells have reduced chemotaxis to cAMP (Yan *et al.*, 2012). Wiskott–Aldrich syndrome protein (WASP) is an actin nucleation–promoting factor that activates the Arp2/3 complex to form branched actin filaments for pseudopod extension (Myers *et al.*, 2005). Disruption of one of the copies of *Dictyostelium* WASP (*wasA*) causes a decrease in chemotaxis toward cAMP (Myers *et al.*, 2005). The Rho GTPase RacC regulates activation of WASP to potentiate polarized F-actin formation during cAMP chemotaxis (Han *et al.*, 2006). In contrast, loss of *wasA* does not affect chemotaxis toward folate (Davidson *et al.*, 2018). Another actin nucleation–promoting factor that activates the Arp2/3 complex is a WASP-related protein called suppressor of cAR (SCAR). *scrA*$^-$ cells and cells lacking NapA, a component of the SCAR complex, show normal chemotaxis toward cAMP (Ibarra *et al.*, 2006). Although *elmoE*$^-$, *wasA*$^-$, and *napA*$^-$ cells moved away from AprA, *racC*$^-$ and *scrA*$^-$ cells did not (Figure 1A). A cAMP gradient causes Ras to activate downstream proteins including Rho GTPases (Affolter and Weijer, 2005). In starved cells, cAMP causes phosphorylation of Ser71 of RacC as detected by an anti-Cdc42/Rac1-phospho-Ser71 antibody (Schwarz *et al.*, 2012). AprA did not have a significant effect on levels of phosphorylated RacC (Supplemental Figure S6B). Together, these data indicate that some but not all components of the machinery that regulates the actin cytoskeleton are necessary for AprA chemorepulsion, and that although AprA requires RacC to induce chemorepulsion, AprA does not affect RacC phosphorylation at the Ser71 site.

AprA does not affect persistence or speed of mutant cells

To further understand the mechanism by which AprA affects cell movement, we examined the persistence of cell movement using the data from Figure 1A. Persistence is the Euclidean distance between the start and end point of a cell's movement divided by the integrated distance traveled by the cell. Cells have a greater persistence when they move directly from start to end points, while cells have a lower persistence when they move randomly. Persistence thus characterizes the straightness of cell movement. In the 0–300 ng/ml AprA gradients used in this report, neither wild-type cells nor any of the mutants examined showed a change in persistence of movement in an AprA gradient compared with no gradient (Figure 1B and Supplemental Figure S2B). This indicates that over a period of 40 min, for cells that did exhibit chemorepulsion from AprA, cells tended to move to an end point with roughly the same persistence (track straightness) whether or not there was an AprA gradient, but when there was an AprA gradient, the tracks tended to be directed away from AprA. As previously observed, some mutants appeared to have inherent changes in persistence of cell movement (Han *et al.*, 2006; Bosgraaf and Van Haastert, 2009; Para *et al.*, 2009; Yan *et al.*, 2012; Scavello *et al.*, 2017). Together, these results suggest that AprA mediates chemorepulsion without changing persistence of cell movement. The maximum concentration of accumulated AprA for cells in shaking culture is 300 ng/ml (Choe *et al.*, 2009). We previously observed a significant increase in the directional persistence of wild-type cells in a 0–2 µg/ml AprA gradient compared with cells in no gradient (Phillips and Gomer, 2012), suggesting that cells increase directional persistence if the AprA concentration exceeds physiological concentrations.

During cAMP-mediated chemoattraction, cell speeds tend to increase (Scavello *et al.*, 2017). To examine whether AprA mediates chemorepulsion by changing the speed of a cell, we used the data from Figure 1A to examine cell speeds. Speed is the path length traveled by a cell divided by the time taken to travel that path. As previously observed for wild-type AX2 (Phillips and Gomer, 2012), AprA did not significantly affect the speed of wild-type or mutant cells, although several mutants had decreased speed in the presence or absence of AprA (Figure 1C and Supplemental Figure S2C). Together, these results indicate that AprA mediates chemorepulsion without changing cell speed, and that as previously observed for some of the mutants where speed was measured for starved cells in a cAMP gradient (Myers *et al.*, 2005; Han *et al.*, 2006; Ibarra *et al.*, 2006; Bosgraaf and Van Haastert, 2009; Para *et al.*, 2009; Scavello *et al.*, 2017), some of the mutants have an inherent decrease in speed.

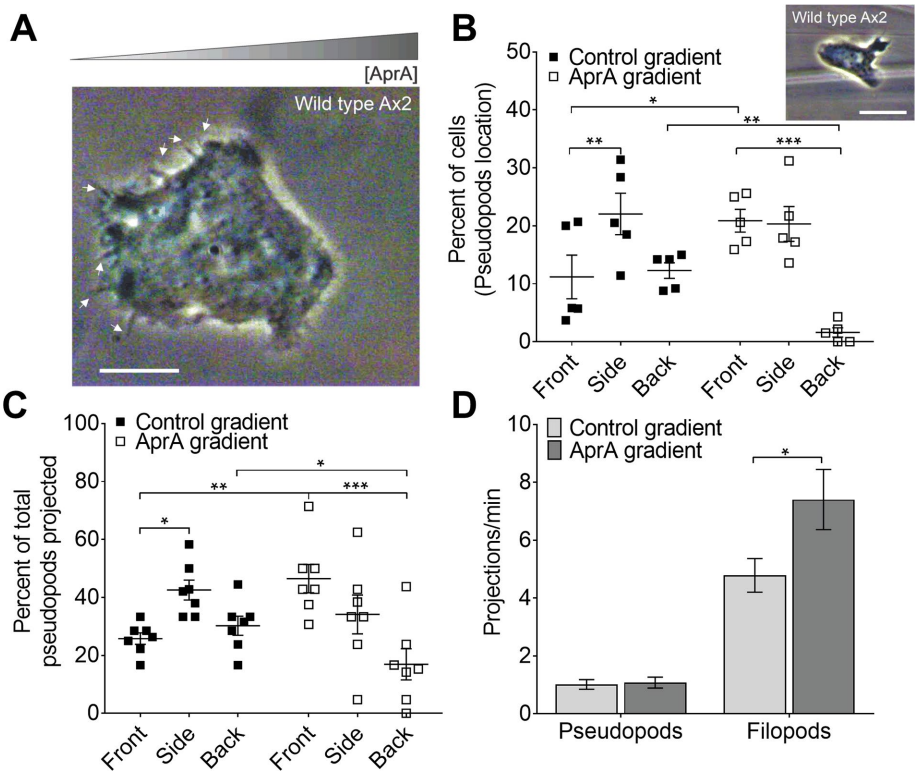

FIGURE 3: AprA enhances pseudopod formation at the front and inhibits pseudopod formation at the back of cells. (A) A wild-type AX2 cell in an AprA gradient. Arrows indicate protruded filopods. The image was taken using a 1.4 NA 60× oil objective; bar is 5 μm. (B) From images of at least 30 cells per experiment, the percent of cells with a discernible pseudopod at the front (the side of the cell away from the AprA source), sides, or back (the side of the cell closest to the AprA source) in the presence or absence of an AprA gradient was calculated. Each point represents the average of the ≥30 cells for each of five independent experiments. Lines represent mean ± SEM of the five averages. A wild-type AX2 cell showing a pseudopod is shown; bar is 10 μm. (C) Approximately 30 cells per experiment were imaged for 140 s; pseudopods were scored as forming at the front, sides, or back; and the percent of pseudopods in these locations was then calculated. Each point represents the average of the 30 cells for each of seven independent experiments. Lines represent mean ± SEM of the seven averages. (D) Quantification of pseudopod and filopod projections per minute in the presence or absence of an AprA gradient, imaging at least 13 cells per experiment. The data represent mean ± SEM of all of the cells from three independent experiments. * indicates $p < 0.05$, ** indicates $p < 0.01$, and *** indicates $p < 0.001$ (two-way ANOVA; Fisher's LSD test for B and C and a *t* test for D).

expected for a random distribution of pseudopod directions, the percent of cells with pseudopods at the front was similar to the percent of cells with pseudopods at the back, and there were roughly twice as many cells with pseudopods at the sides. In AprA gradients, the percent of cells with pseudopods at the front was increased, the percent of cells with pseudopods at the back was sharply decreased, and the percent with pseudopods at the side was similar to the control (Figure 3B). Similar results were obtained using videomicroscopy to examine pseudopod protrusions over 20 min in wild-type AX2 and NC4 cells (Figure 3C and Supplemental Figure S7A). Despite changing the location of pseudopods, the presence of an AprA gradient did not significantly change the overall frequency of pseudopod projections of both wild-type AX2 and NC4 cells, but did cause an increase in the frequency of filopod projections of AX2 cells (Figure 3D and Supplemental Figure S7B). AprA gradients did not significantly affect the size of the pseudopods, the length of the filopods, the lifespan of the pseudopods, or the lifespan of the filopods, and in the presence or absence of an AprA gradient, there was a similar weak trend toward increased pseudopod lifetime with increased pseudopod length (Supplemental Figures S8, A–E, and S7C). Together, these results suggest that similar to the chemoattractant cAMP, AprA causes cells to decrease pseudopod formation at the back of a cell and increase pseudopod formation at the front of a cell. However, unlike steep cAMP gradients, which increase the overall pseudopod formation rate compared with no gradient, and like shallow cAMP gradients, which do not increase pseudopod formation (Bosgraaf and Van Haastert, 2009; Van Haastert, 2010), AprA gradients do not increase the rate of pseudopod formation. These results were observed for both axenic (AX2) and nonaxenic (NC4) cells.

An AprA gradient shifts pseudopod formation from the rear to the front of a cell without changing the frequency of pseudopod formation

Depending on the nature of the gradient, there can be increased pseudopod and filopod formation at the front of a cell during chemoattraction (Heid *et al.*, 2005), or no increase in pseudopods (Bosgraaf and Van Haastert, 2009). To determine whether chemorepulsion from AprA causes increased pseudopod formation, we examined the morphology of wild-type AX2 and NC4 cells in an AprA gradient (Figure 3, A–D, and Supplemental Figure S7, A–C). Imagining the gradient going east-west, with the AprA source to the west, we considered the front of a cell to be the 90° sector extending from northeast to southeast, the back of the cell to be the sector extending from northwest to southwest, and the sides to be the combination of the remaining two 90° sectors. In the absence of a gradient, we used the same sectors to define an arbitrary front, back, and sides irrespective of the direction of cell movement. In the absence of a gradient, approximately half of the wild-type AX2 cells at any given time had a discernable pseudopod (Figure 3B). As

Unlike cAMP, AprA does not increase cytoskeletal actin and myosin II

cAMP induces starved wild-type cells to rapidly increase the amount of actin and myosin II in the detergent-insoluble cytoskeleton (Supplemental Figure S9, B and D; Dharmawardhane *et al.*, 1989). To determine whether AprA has a similar effect on the cytoskeleton of vegetative cells, we incubated wild-type cells with AprA and assayed for total actin and myosin II as well as actin and myosin II in the cytoskeleton for up to 12 h to examine the possible long-term effects of AprA (AprA appears to form a relatively time-invariant gradient compared with the rapid pulses of cAMP that induce chemoattraction). Like cAMP, AprA did not significantly affect levels of total actin and total myosin II, but unlike cAMP, AprA did not significantly affect levels of cytoskeletal actin or cytoskeletal myosin II (Figure 4, A–D, and Supplemental Figure S9, A–D).

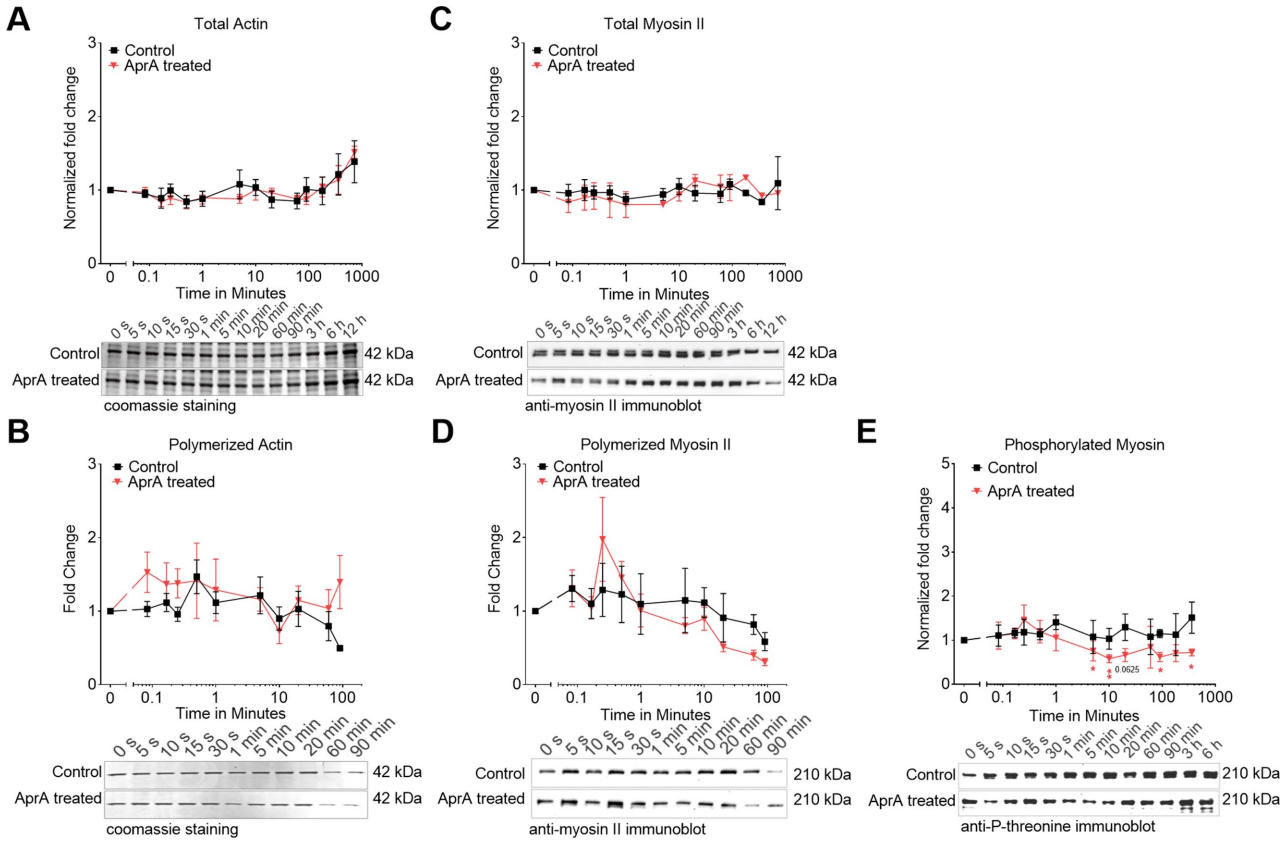

FIGURE 4: AprA does not significantly affect levels of polymerized actin or myosin II. Cells were incubated in growth medium with AprA or an equivalent amount of buffer for the indicated amounts of time, and whole cell lysates (A, C, and E) or detergent-insoluble cytoskeletons (B and D) were run on SDS–polyacrylamide gels. Gels were stained with Coomassie (A, B), or Western blots of the gels were stained with anti-myosin II antibodies (C, D), or anti-P-threonine antibodies (E). Densitometry was used to estimate levels of actin (A, B), myosin II (C, D), or phosphorylated myosin (E). For B, polymerized actin densitometry was normalized to the total actin (A) densitometry for each timepoint. For C and E, polymerized myosin II and phosphorylated myosin densitometry was normalized to the total myosin II (C) densitometry for each timepoint. Values are mean ± SEM for 3 (C), 4 (A, D, and E), or 5 (B) independent experiments. * indicates $p < 0.05$ and ** indicates $p < 0.01$ (*t* test with Welch's correction). Images show representative staining for each experiment.

In cell movement, myosin II stabilizes the cytoskeleton by associating with the actin meshwork, and provides force on actin filaments (Levi *et al.*, 2002). Myosin II is active in its filamentous form, which is negatively regulated by phosphorylation (Liang *et al.*, 1999). During chemoattraction to cAMP, one report showed no significant change in the level of phosphorylated myosin (Berlot *et al.*, 1985), while another showed a 1.6-fold increase in myosin phosphorylation (Dembinsky *et al.*, 1997). In agreement with Berlot *et al.* (1985), we observed that cAMP did not change the level of phosphorylated myosin (Supplemental Figure S9E). In contrast, AprA caused a slight decrease in phosphorylated myosin II starting at 5 min (Figure 4E). These results indicate that unlike cAMP, AprA does not increase levels of cytoskeletal actin and myosin, and also unlike cAMP, AprA decreases levels of phosphorylated myosin II.

Cells that are unresponsive to AprA do not form actin-rich pseudopods at the front of the cell

To move toward cAMP, *Dictyostelium* cells rapidly increase the amount of polymerized actin (F-actin) at the leading edge by locally activating signaling cascades (Sasaki *et al.*, 2004). To determine whether mutants that are defective in AprA-induced chemorepulsion affect actin polymerization, we exposed cells to an AprA gradient and stained for F-actin. As before, we defined the leading edge of a cell in an AprA gradient as the 25% of the cell periphery on the side away from the source of AprA, and for cells in no gradient, we used the same sector of a cell, irrespective of the direction that the cell was moving in. As previously observed, AprA induced F-actin formation at the leading edge of wild-type cells (Figure 5A; Phillips and Gomer, 2012). Many of the mutants that moved away from AprA (*rasG*$^-$, *docA*$^-$, *pkbA*$^-$, *pkbA*$^-$/*pkgB*$^-$, *gca*$^-$/*sgcA*$^-$, and *elmoE*$^-$) also showed a significant increase in the number of cells with F-actin at the leading edges in AprA gradients compared with the cells in the control (Figure 5B). In contrast, we did not observe any changes in localization of F-actin in those mutant cells that did not move away from AprA (Figures 1 and 5B). Together these data suggest that mutants that are not repelled by AprA (Figure 1) also do not show more F-actin in the sector of the cell facing away from AprA.

AprA requires PakD and SCAR to regulate Ras

p21-Activated kinase D (PakD) regulates actin assembly, is necessary for cAMP chemoattraction, and localizes to cell protrusions in starved cells (Garcia *et al.*, 2014). We previously observed that PakD localizes to a punctum in a motile cell, and that loss of PakD abolishes AprA-mediated chemorepulsion (Phillips and Gomer, 2014). To determine whether AprA affects the location of PakD, we analyzed the PakD localization in *pakD*$^-$ cells expressing PakD-GFP

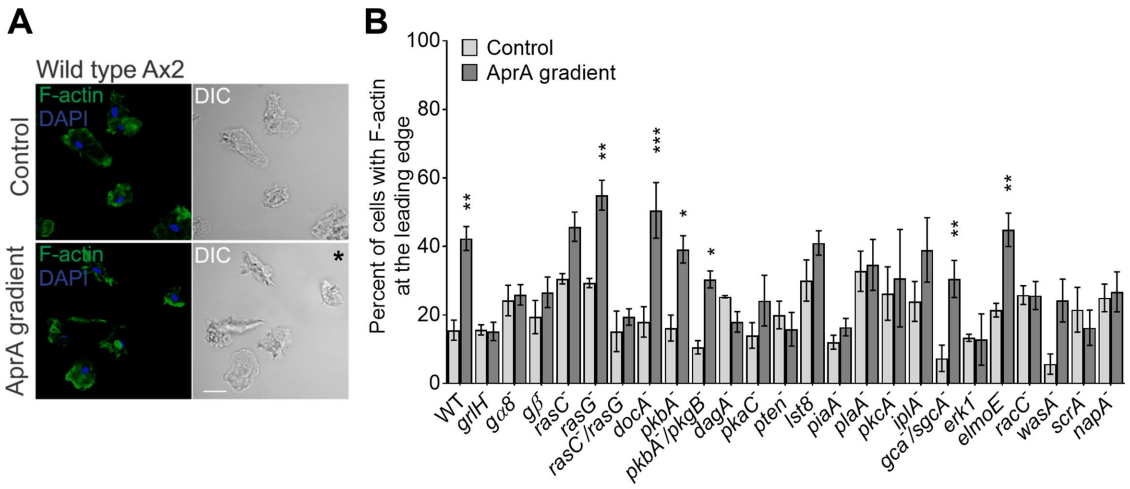

FIGURE 5: AprA causes a localization of F-actin in *Dictyostelium* cells. (A) Localization of F-actin in wild-type cells incubated in an AprA gradient for 20 min, fixed, and stained with phalloidin 488 (green) for F-actin and the DNA dye DAPI (blue). DIC represents differential interference contrast. Image is representative of three independent experiments. * indicates that the source of the rAprA was above and to the right of the figure; bar is 10 μm. (B) Quantification of cells with F-actin at the leading edge in AprA gradients or no gradient (control), fixed and stained with phalloidin 488. For each experiment, at least 30 cells were examined and the percent of cells with F-actin localized at the edge away from the AprA source was calculated. Values are mean ± SEM of the percentages of cells from three independent experiments. * indicates $p < 0.05$, ** indicates $p < 0.01$, and *** indicates $p < 0.001$ compared with control for the indicated genotype (*t* tests).

(Phillips and Gomer, 2014). Compared to controls, AprA induced a significant increase of cells with detectable PakD-GFP puncta, and these puncta did not colocalize with F-actin or myosin II (Figure 6, A and B). These data suggest that AprA affects PakD puncta.

In mammalian cells, Pak kinases appear to regulate Ras, and Ras appears to regulate Paks (Tang *et al.*, 1999; Sun *et al.*, 2000). To determine whether PakD regulates Ras activation during chemorepulsion, we examined whether *pakD*⁻ cells exhibit translocation of RBDRaf1-GFP to the cell cortex. In the absence of AprA, the percent of *pakD*⁻ cells with cortical RBDRaf1-GFP was approximately the same as the percent of AprA-treated wild-type cells with cortical RBDRaf1-GFP, and AprA did not significantly affect RBDRaf1-GFP localization in *pakD*⁻ cells (Figure 2, B and C). These data suggest that PakD negatively regulates Ras activation.

During chemotaxis to cAMP, a feedback loop involving F-actin and $PI(3,4,5)P_3$ affects Ras activation (Sasaki *et al.*, 2004). To examine whether the actin cytoskeleton plays a similar role in Ras activation during chemorepulsion, we examined the translocation of RBDRaf1-GFP in *scrA*⁻ cells. We did not observe cortical RBDRaf1-GFP in control or AprA-treated *scrA*⁻ cells (Supplemental Figure S4B). These results indicate that AprA requires SCAR to induce RBDRaf1-GFP translocation to the cell cortex and thus Ras activation.

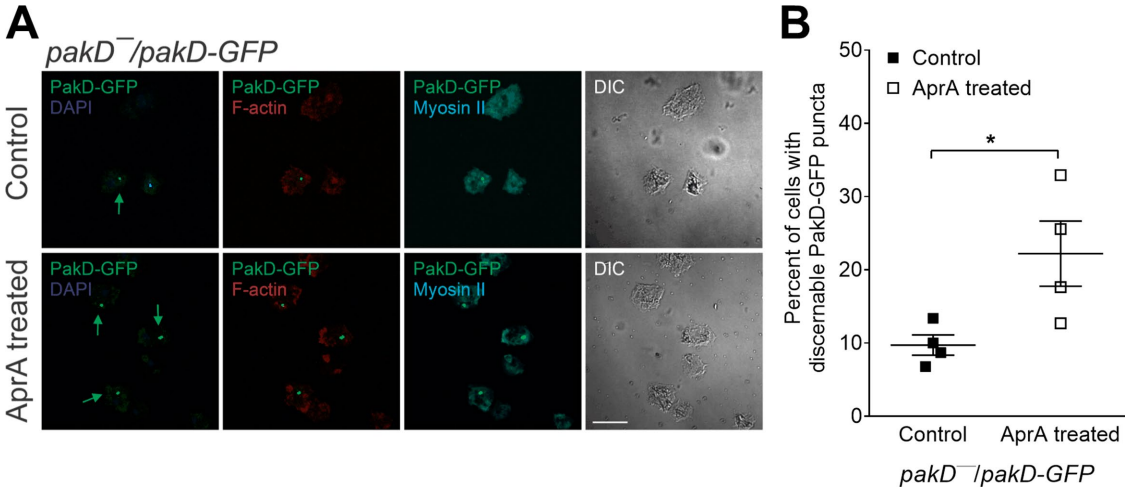

FIGURE 6: AprA induces translocation of PakD. (A) Localization of ectopically expressed PakD-GFP in *pakD*⁻ cells incubated in growth medium with AprA or an equivalent volume of buffer (control) for 20 min, fixed, and stained with phalloidin 555 for F-actin (red), anti-myosin II (cyan), and the DNA dye DAPI (blue). Arrows in A indicate PakD-GFP puncta within the cells. DIC represents differential interference contrast; bar is 10 μm. (B) Quantification of PakD-GFP puncta in those cells. Quantitation of PakD-GFP puncta was analyzed by observers blinded to whether cells were exposed to exogenous AprA or not. Images are representative of, and data are mean ± SEM of, four independent experiments. * indicates $p < 0.05$ (paired *t* test).

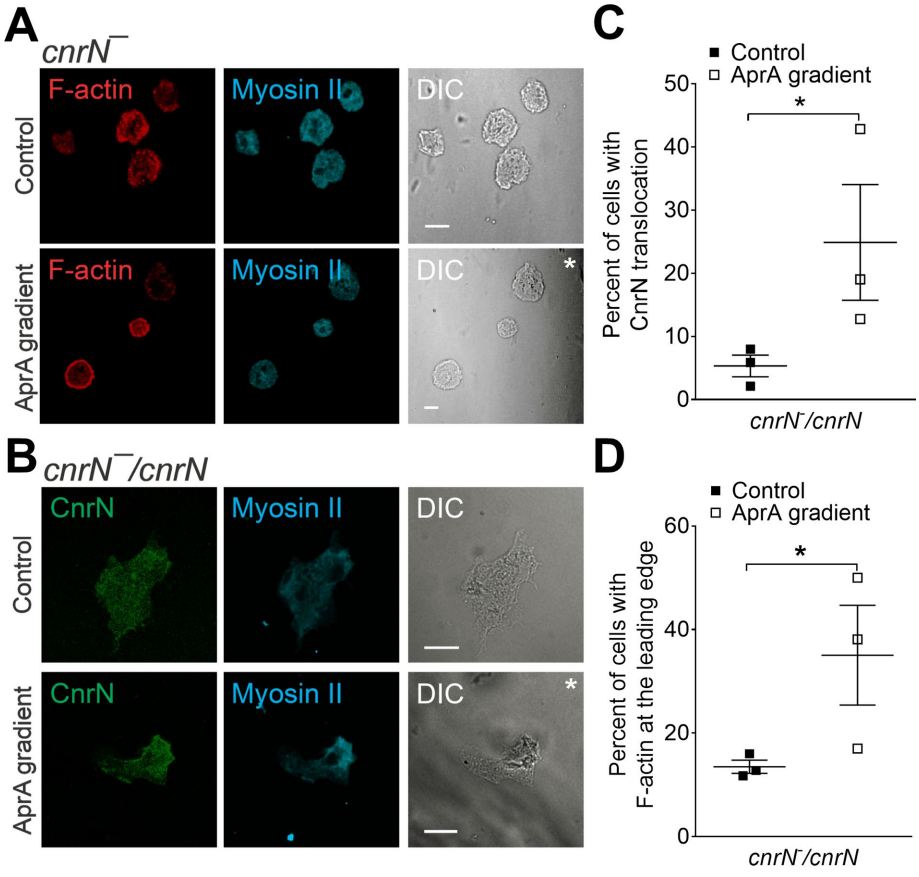

FIGURE 7: AprA causes the PTEN-like protein CnrN to translocate to the back of cells. (A, B) *cnrN*⁻ and *cnrN*⁻ cells ectopically expressing myc-tagged CnrN (*CnrN*⁻*/CnrN*) were incubated in the presence or absence (control) of an AprA gradient for 20 min, fixed, and stained with phalloidin 555 for F-actin (red), anti-myosin II (cyan), or anti-myc (green). Images are representative of cells from three independent experiments. * indicates that the source of AprA was above and to right of the image and the direction of cell movement was down the AprA gradient (toward the lower left). DIC: differential interference contrast; bars are 10 μm. (C) Approximately 80 cells from B were scored for CnrN translocation to the rear of the cell, and the percent of cells with CnrN translocation was calculated. Scores were generated by blinded observers. Values are mean ± SEM of the percentages from three independent experiments. (D) The percent of *CnrN*⁻*/CnrN* cells with F-actin at the leading edge was scored as in C. Values are mean ± SEM of the percentages from three independent experiments. * indicates $p < 0.05$ (paired *t* test).

CnrN maintains cell polarity during AprA chemorepulsion

CnrN is a PTEN-like phosphatase that regulates phosphatidylinositol 3,4,5-trisphosphate (PIP3) levels during chemotaxis toward cAMP (Tang and Gomer, 2008). In starved cells moving toward cAMP, PTEN accumulates at the rear of the cell and dephosphorylates PIP3, preventing pseudopod formation at the rear (Iijima and Devreotes, 2002; Wessels *et al.*, 2007). Loss of CnrN blocks AprA-induced chemorepulsion (Herlihy *et al.*, 2013b). In *cnrN*⁻ cells, AprA gradients caused enrichment of F-actin at the cell cortex but did not cause an enrichment of F-actin or myosin II at one side or another of the *cnrN*⁻ cells (Figure 7A), and this response was rescued by expressing CnrN in the *cnrN*⁻ cells (Figure 7, B–D). Using Western blots to analyze crude cytosol and crude membrane/cytoskeleton fractions, we previously found that AprA causes an increase in membrane and/or cytoskeleton-associated myc-tagged CnrN expressed in *cnrN*⁻ cells (Herlihy *et al.*, 2013b). We observed that the myc-CnrN localized to the rear of *cnrN*⁻ cells and approximately colocalized with myosin II in AprA gradients (Figure 7, B and C). These results suggest that AprA causes a translocation of CnrN to the rear of cells and that CnrN is necessary for the biased cell cortex enrichment of F-actin and/or myosin II during AprA-mediated chemorepulsion.

DISCUSSION

We used different *Dictyostelium* knockout strains to compare the signal transduction pathways utilized by the *Dictyostelium* chemorepellent AprA to the chemoattractant cAMP signal transduction pathways. Some genes that are involved in chemoattraction to cAMP are necessary for chemorepulsion from AprA, while other genes that are involved in chemoattraction to cAMP do not appear to be necessary for chemorepulsion from AprA (Figure 8). A possible reason that the AprA chemorepulsion mechanism does not need some of the genes that are necessary for chemoattraction to cAMP is that chemorepulsion may require less directional accuracy than attraction to a point. In steep but not shallow cAMP gradients, activation of the cAMP signal transduction pathways induces actin polymerization and the formation of new pseudopods. Possibly as a result of AprA not using several of these pathway components, AprA does not induce actin polymerization or the formation of new pseudopods, but instead simply inhibits pseudopod formation at the side of the cell closest to the source of AprA. Like chemorepulsion from AprA, chemoattraction to folate does not require many of the cAMP signaling components, suggesting that some basic signal transduction pathways are sufficient to induce cell migration in gradients of attractants and repellents.

The beginning of the cAMP chemoattraction pathway involves a G protein–coupled receptor activating G proteins and Ras, and AprA uses the G protein–coupled receptor GrlH, and the G proteins Gα8 and Gβ (Phillips and Gomer, 2012; Tang *et al.*, 2018). The AprA-related neutrophil chemorepellent DPPIV also uses a G protein–coupled receptor to repel cells (White *et al.*, 2018). cAMP pulses cause Ras to be activated within 1 min, and deactivated within 2–3 min (Kortholt *et al.*, 2011). We found that Ras is also necessary for, and activated by, AprA signaling. Ras was activated at both 5 and 20 min after adding AprA, indicating a much slower, if any, deactivation process. Both axenic cells (with high macropinocytosis) and NC4 cells (with normal macropinocytosis) were repelled by AprA, indicating that abnormally high levels of macropinocytosis do not interfere with AprA-mediated chemorepulsion (Veltman *et al.*, 2014; Bloomfield *et al.*, 2015). PakD and SCAR affect the ability of AprA to activate Ras, indicating that either other external signals or internal conditions modulate chemorepulsion, or that feedback loops amplify or attenuate chemorepulsion.

cAMP chemoattraction uses at least six pathways downstream from the cAMP receptor (Ma *et al.*, 1997; Kortholt *et al.*, 2011;

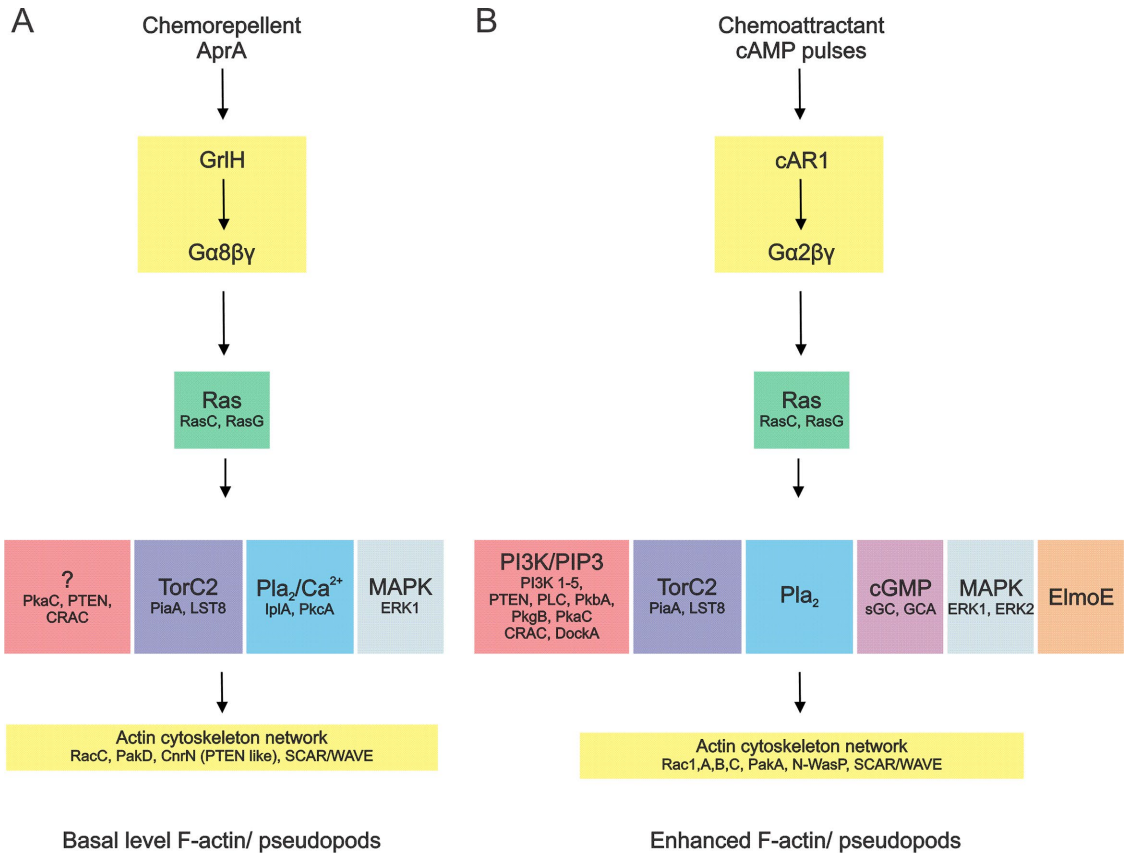

FIGURE 8: Working model for chemorepulsion and chemoattraction signal transduction pathways. (A) The chemorepellent AprA signals through the GrlH G protein–coupled receptor, and G proteins Gα8, Gβ, and Gγ. AprA requires GrlH to activate Ras, which possibly activates TorC2, Pla_2/Ca^{2+}, MAPK, and some components of PI3K signaling to regulate actin cytoskeleton network proteins such as RacC, PakD, CnrN, and SCAR/WAVE during cell movement without inducing F-actin and pseudopod formation. (B) cAMP pulse–induced signaling pathways, which include cAR1 G protein–coupled receptor, G proteins Gα2, Gβ, and Gγ. cAMP activates Ras and other signaling pathways such as PI3K/PIP3, TorC2, Pla_2, cGMP, MAPK, and ElmoE and cause actin cytoskeleton proteins such as Rac1, PakA, N-WasP, and SCAR/WAVE to induce enhanced F-actin and pseudopods.

Yan *et al.*, 2012). AprA chemorepulsion appears to use components of the TorC2, phospholipase A/Ca^{2+}, and MAP kinase pathways. Although AprA chemorepulsion requires the MAP kinase pathway component ERK1, AprA does not appear to affect ERK1 phosphorylation at the Thr202/Tyr204 site, suggesting either that AprA chemorepulsion simply requires a basal level of ERK1 activity or that AprA regulates ERK1 at a different site.

AprA chemorepulsion does not appear to use components of the cyclic GMP, ElmoE, and PI3 kinase pathways. Although a chemorepellent cAMP analogue requires PI3 kinase and phospholipase C, AprA chemorepulsion does not require PI3 kinases 1 and 2 or phospholipase C (Keizer-Gunnink *et al.*, 2007; Phillips and Gomer, 2012) and here we also found that other components of PI3 kinase signaling such as Akt/PKB homologues PkbA and PkgB, and Dock-like protein (DockA) are not necessary for AprA chemorepulsion. In addition to being activated by PI3 kinase activity, Akt/PKB is also activated by TorC2 (Kamimura *et al.*, 2008). However, AprA did not discernibly affect the phosphorylation of Akt/PKB substrates, suggesting that Akt/PKB and its downstream targets are not involved in the AprA signaling pathway.

Although the Ca^{2+} channel IplA is not important for cAMP chemoattraction (Traynor *et al.*, 2000), IplA is necessary for AprA chemorepulsion, indicating that there exist pathways used for AprA chemorepulsion that are not used by cAMP.

PTEN and the PTEN-like phosphatase CnrN are necessary for chemorepulsion from AprA, and AprA causes CnrN to accumulate at the rear of cells. Together, these observations suggest that CnrN is part of the AprA signal transduction pathway. Both phosphatases decrease levels of PIP3 (Comer and Parent, 2002; Tang and Gomer, 2008). Although Akt/PKB is regulated by PIP3, we did not see a statistically significant effect of AprA on Akt/PKB activity as measured by phosphorylation of Akt/PKB substrates. One possible explanation for this is that AprA activates PTEN and CnrN, and the resulting effect of presumably decreased levels of PIP3 at the rear of cells is too subtle to be detected by, or is undetected by, our phosphorylation of Akt/PKB substrate assays. A second possible explanation is that PTEN and CnrN are used for some function in AprA chemorepulsion that does not involve dephosphorylating PIP3. A third possible explanation is that AprA activates PTEN and CnrN, decreasing PIP3 levels, and some other part of the pathway blocks Akt/PKB activity.

Chemotaxis involves regulation of the actin cytoskeleton. In *Dictyostelium*, the small GTPase Rac activates SCAR, which in turn activates the key actin nucleation factor Arp2/3 (Eden *et al.*, 2002). As previously observed for cAMP chemoattraction (Veltman *et al.*, 2012), we found that the loss of RacC or SCAR caused a defect in AprA chemorepulsion. AprA did not significantly affect RacC phosphorylation at the Ser71 site, suggesting that either the basal level

activity of RacC is sufficient to activate actin polymerization or that AprA activates Rac at a different site (Schwebs and Hadwiger, 2015).

In starved cells, cAMP increases levels of polymerized actin and myosin II (Dharmawardhane *et al.*, 1989), and cAMP either increases or has no effect on phosphorylation of the myosin II heavy chain (MHC II; Berlot *et al.*, 1985; Dembinsky *et al.*, 1997). We observed that cAMP did not affect MHC II phosphorylation, suggesting that subtle changes in culture conditions among labs affects cAMP-induced MHC II phosphorylation in starved cells. In vegetative cells, AprA did not significantly affect levels of polymerized actin and myosin II, and decreased MHC II phosphorylation. Because dephosphorylation of MHC II causes it to polymerize (Ravid and Spudich, 1989), one possible explanation for decreased MHC II phosphorylation having no effect on MHC II polymerization is that the myosin is already mostly polymerized in vegetative cells. In agreement with the lack of an effect of AprA on actin and myosin II polymerization, there was no effect of AprA on the frequency of pseudopod formation, and AprA simply decreased pseudopod formation at the rear of cells to induce chemorepulsion. Because there exist chemorepellents in higher eukaryotes (Herlihy *et al.*, 2013a, 2015, 2017; de Oliveira *et al.*, 2016; Nourshargh *et al.*, 2016; White *et al.*, 2018), an intriguing possibility is that they also use a simple mechanism to induce directional cell movement.

MATERIALS AND METHODS

Cell strains and culture

Dictyostelium discoideum strains were obtained from the *Dictyostelium* Stock Center (Fey *et al.*, 2013) and were wild-type AX2, *grlH*$^-$ (DBS0350226; Tang *et al.*, 2018), *gα8*$^-$ (DBS0236107; Wu *et al.*, 1994), *gβ*$^-$ (DBS0236531; Lilly *et al.*, 1993; Wu *et al.*, 1995; Peracino *et al.*, 1998), *rasC*$^-$ (DBS0236853; Lim *et al.*, 2001), *rasG*$^-$ (DBS0236862; Bolourani *et al.*, 2006), *rasC*$^-$/*rasG*$^-$ (DBS0236858; Bolourani *et al.*, 2006), *plaA*$^-$ (DBS0238068; Chen *et al.*, 2007), *iplA*$^-$ (DBS0236260; Traynor *et al.*, 2000), *docA*$^-$ (DBS0252716; Santorelli *et al.*, 2008), *elmoE*$^-$ (DBS0350065; Yan *et al.*, 2012), *dagA*$^-$ (DBS0235559; Lilly and Devreotes, 1995), *pkbA*$^-$ (DBS0349876; Tang *et al.*, 2011), *pkbA*$^-$/*pkgB*$^-$ (DBS0236785; Meili *et al.*, 2000), *piaA*$^-$ (DBS0349879; Tang *et al.*, 2011), *lst8*$^-$ (DBS0236517; Lee *et al.*, 2005), *pkcA*$^-$ (DBS0350916; Mohamed *et al.*, 2015), *gca*$^-$/*sgcA*$^-$ (DBS0302679; Roelofs *et al.*, 2001), *scrA*$^-$ (DBS0236926; Blagg *et al.*, 2003), *pkaC*$^-$ (DBS0236783; Mann and Firtel, 1991), *wasA*$^-$ (a gift from Robert Insall, Beatson Institute for Cancer Research, Glasgow, UK; Davidson *et al.*, 2018), *pakD*$^-$ (DBS0350281; Garcia *et al.*, 2014), *cnrN*$^-$ (DBS0302655; Tang and Gomer, 2008), *racC*$^-$ (Wang *et al.*, 2013), *pakD*$^-$/*pakD-GFP* (DBS0350395; Phillips and Gomer, 2014), *cnrN*$^-$/*cnrN-Myc* (DBS0302656; Tang and Gomer, 2008), *erk1*$^-$ (DBS0350622; Nguyen *et al.*, 2010), and *pten*$^-$ (DBS0236830; Iijima and Devreotes, 2002). Cells were grown at 21°C in shaking culture in HL5 medium and in SM/5 agar with lawn of *Escherichia coli* B/R20 (*Dictyostelium* Stock Center) and 100 µg/ml dihydrostreptomycin and 100 µg/ml ampicillin were used to kill *E. coli* in *Dictyostelium* cultures obtained from SM/5 agar (Brock and Gomer, 1999). Cells expressing a selectable marker were grown under selection with the appropriate antibiotics and supplements (5 µg/ml blasticidin, 5 µg/ml neomycin sulfate, 100 µg/ml thymidine, 20 µg/ml uracil, and/or 25 µg/ml hygromycin). The plasmid pDm-115RafRBD (a kind gift from Wouter-Jan Rappel; Kortholt and van Haastert, 2008) encoding the RBD of Raf1 was used to transform wild-type AX2, *pakD*$^-$, and *scrA*$^-$ cells by electroporation (Shaulsky *et al.*, 1996) to generate the strains AX2/*RBDRaf1-GFP*, *pakD*$^-$/*RBDRaf1-GFP*, *scrA*$^-$/*RBDRaf1-GFP*, and *grlH*$^-$/*RBDRaf1-GFP*. Cells were grown under constant selection and the expression of RBDRaf1 was confirmed by immunofluorescence imaging of the fixed cells as described below.

Diffusion calculation

The theoretical concentration of AprA at various distances from the center of a disk of cells was calculated following Yuen and Gomer (1994) for a 3.79-mm-radius disk of cells in a square grid with 10 µm center-to-center spacing (essentially confluent). The diffusion coefficient (3×10^7 cm^2/s) was calculated for the 55 kDa AprA, adjusting for diffusion on moist dirt or on agar (Yuen and Gomer, 1994) using a secretion flux of 2.6×10^{-8} ng AprA/cell per min (Choe *et al.*, 2009).

Reverse transcription (RT-PCR) analysis

To verify the genotype of strains, total RNA was isolated from wild-type AX2 and mutant strains using a QuickRNA miniprep kit (Zymoresearch) and cDNA was generated using a Maxima H minus first strand synthesis kit (Thermo Fisher). PCR with gene-specific primers was then used to verify loss of the cDNA associated with a gene disruption (Supplemental Figure S10 and Table 1) using specific primer pairs for each gene, and a primer pair for glyceraldehyde 3-phosphate dehydrogenase (*gpdA*) as a positive control (Brock and Gomer, 1999).

Recombinant AprA, proliferation inhibition, and chemorepulsion assays

Recombinant AprA (rAprA) was expressed in *E. coli*, purified, and checked for purity as described previously (Brock and Gomer, 2005). The rAprA was resuspended in 20 mM $NaPO_4$, pH 7.4, to typically 250 µg/ml. The rAprA was tested for proliferation inhibition and chemorepulsion activity before use for further experiments. Proliferation inhibition was measured as previously described (Bakthavatsalam *et al.*, 2009). Chemorepulsion activity in terms of FMI and speed was measured in Insall chambers as previously described (Muinonen-Martin *et al.*, 2010; Phillips and Gomer, 2012), with HL5 in the center control well and 300 ng/ml rAprA (diluted from the stock in 20 mM $NaPO_4$) in HL5 in the outer well (White *et al.*, 2015). At least 10 cells per experiment were tracked by a blinded observer every 15 s for 40 min. As a control, cells were tracked as above but with a volume (equal to the volume of AprA added to the HL5 for the gradient experiment) of 20 mM $NaPO_4$, pH 7.4, added to the HL5 in the outer well. The persistence of cell movement was measured as the directedness of cell movement in the AprA gradient irrespective of the direction of gradient and was calculated as previously described for directionality (Phillips and Gomer, 2012). The chemorepulsion assay for each strain (in the presence and absence of an AprA gradient) was repeated at least two times for a total of at least three independent replicates.

Imaging of cells in AprA gradients

Dictyostelium cells at 8×10^4 cells/ml in HL5 were grown overnight in type 354118 eight-well slides (Corning, Big Flat, NY) with 300 µl/well in a metal egg poacher filled with water to generate an approximately isothermal environment to minimize convection currents. Recombinant AprA (1.8 µl of 50 µg/ml) was added very gently to the top right corner of each well. After 20 min, the medium was gently removed using a pipette tip at the top right corner of the well. Cells were fixed with 4% wt/vol of paraformaldehyde (Electron Microscopy Sciences, Hatfield, PA) in phosphate-buffered saline (PBS) for 10 min, washed once with PBS, and permeabilized with 0.1% Triton X-100 (Alfa Aesar, Tewksbury, MA) in PBS for 5 min. Cells were washed with PBS twice, blocked with 1 mg/ml type 0332 bovine serum albumin (VWR, Solon, OH) in PBS for 1 h and washed once with PBS. Cells

grlH Forward: 5′-TCTAGCCAAGGTCATACTGTCGC-3′	*gcA* Reverse: 5′-CCCACGACACCAGCAATAACAGG-3′
grlH Reverse: 5′-AGATCGTTGGTGGCTCTTTCGG-3′	*sgcA* Forward: 5′-GGCTCTAACAGTGGAAGGTTGTGC-3′
rasC Forward: 5′-AGCCGGTCAAGAAGAGTATAGCG-3′	*sgcA* Reverse: 5′-GGGGACAGTGACAGCAGTAGCA-3′
rasC Reverse: 5′-CCCCTTTTCTTTGGTGGGAGCA-3′	*napA* Forward: 5′-CAACCACCCGCTCCAACCTC-3′
rasG Forward: 5′-GTTGGTGGTGGTGGTGTCGG-3′	*napA* Reverse: 5′-TCAGCATGTTCCTCGGCACG-3′
rasG Reverse: 5′-ACACAAAGGAAACCTTGACCAGTTC-3′	*scrA* Forward: 5′-ACGTGAGCGTAGAGAAGCACG-3′
plaA Forward: 5′-GACGGTGGTGGCACAAAAGG-3′	*scrA* Reverse: 5′-AGAGGATGGTGAAGGGGTGC-3′
plaA Reverse: 5′-GGGTATCAGCTCCATCTGGTGA-3′	*pkaC* Forward: 5′-CGCAGGCGGTGAGGTGTTTAC-3′
iplA Forward: 5′-CGATACCATTGCATTTTGGTGCG-3′	*pkaC* Reverse: 5′-GTGCCCACCAATCGACCGC-3′
iplA Reverse: 5′-CGACAGACAGAGCAAACGCAG-3′	*wasA* Forward: 5′-ACAAATGGTTGGTGGTTCAGCTCC-3′
docA Forward: 5′-AGGTTGGCCAATAGTTTGTCGT-3′	*wasA* Reverse: 5′-TCATTTCTTCCACCGCCGCT-3′
docA Reverse: 5′-CATAAGAGTCACGGCCGCCT-3′	*pakD* Forward: 5′-TCTTCTTCAACGCCACCTCCC-3′
elmoE Forward: 5′-CCATCATATTGGGGGCGGCG-3′	*pakD* Reverse: 5′-GCACATGGTGGTAATGGTGGAG-3′
elmoE Reverse: 5′-GGGGCCACAACAGCTTGAGA-3′	*cnrN* Forward: 5′-ACAGGCTTAGAAGCAAGTTGGAGA-3′
dagA Forward: 5′-CAGCTGTCACTGAAGAGGCAATC-3′	*cnrN* Reverse: 5′-ACGTTGTTGTGAAGGTTGAGTTACA-3′
dagA Reverse: 5′-CACCACCAGTGGCACCAACTC-3′	*gα8* Forward: 5′-CTGACCCCGAAACAAAGAAAAGAGC-3′
pkbA Forward: 5′-GGCGCAGAGATCGTATTGGCA-3′	*gα8* Reverse: 5′-TGACCACCAACATCAACAACACGG-3′
pkbA Reverse: 5′-CCAAGAGGGAACGAGCATCTGG-3′	*gβ*Forward: 5′-CCAACAAAGTCCACGCTATTCCA-3′
pkbR1 Forward: 5′-GGTAAACCCGCCAAAGCAGG-3′	*gβ* Reverse: 5′-GCGGTAGCATCACAAGCACC-3′
pkbR1 Reverse: 5′-GGTGAATCTGGTGAACTTGATGCT-3′	*racC* Forward: 5′-TGCAAACAATCGTTTCCCAGAAGA-3′
piaA Forward: 5′-CGTACTGCTTGTGTAGCATTGGA-3′	*racC* Reverse: 5′-GGCTAAATCGTTACCTTGTTCGGT-3′
piaA Reverse: 5′-CCCTACCAGGCAATTCAGCCA-3′	*gpdA* Forward: 5′-ACCGTTCACGCCATCACTGCC-3′
lst8 Forward: 5′-GCAGCAGCAGGTAACCCACA-3′	*gpdA* Reverse: 5′-GACGGACGGTTAAATCGACGACTG-3′
lst8 Reverse: 5′-TGCAACCACTAAACCACCATCACT-3′	*pten* Forward: 5′-AGTTGCAGTCTCTAAACAAAAGAG-3′
pkcA Forward: 5′-TGGCGTTTCCAGATTCGTAGAGG-3′	*pten* Reverse: 5′-GGTGCGTCTGATGCTACAAC-3′
pkcA Reverse: 5′-CAGGTGGTGGAGTTAGGAGGG-3′	*erk1* Forward: 5′-GCAACTCGTTGGTATCGTGC-3′
gcA Forward: 5′-TGGATTCACTGAAATGGCCGCA-3′	*erk1* Reverse: 5′-TGGATGTGCCAAAGCTTCCT-3′

TABLE 1: Oligonucleotides for genotyping of mutants by PCR.

were incubated with streptavidin blocking solution (Vector Laboratories, Burlingame, CA) for 15 min. Cells were washed once with PBS with 0.1% Tween 20 (PBST; Fisher Scientific, Pittsburgh, PA), incubated with biotin blocking solution (Vector Laboratories, Burlingame, CA), and washed three times with PBST. Primary antibody solution in PBST was added (1:100 mouse monoclonal 3E6cE8 anti-myosin II [a kind gift from David Knecht, University of Connecticut, Storrs, CT]; Knecht and Loomis, 1987), 1:500 rabbit monoclonal anti-Myc tag (Cell Signaling Technology, Danvers, MA), or 1:500 rabbit monoclonal anti-phospho-Akt substrate [RXXS*/T*] (Cell Signaling Technology) and incubated at 4°C overnight. Cells were washed three times with PBST, incubated with 1:500 biotinylated donkey anti-mouse (Jackson ImmunoResearch, West Grove, PA) in PBST for 1 h, washed three times with PBST, incubated with 1:500 Alexa 647 streptavidin (Cell Signaling Technology) or 1:500 Alexa 488 anti-rabbit (Jackson) in PBST for 1 h, and stained with 165 nM of Alexa 488 phalloidin (Thermo Fisher Scientific, Waltham, MA) or 1:2000 ifluor 555 phalloidin (Abcam, Cambridge, MA) in PBS in the dark for 30 min. Cells were washed three times with PBS and dried for 15–20 min, and mounted in Vectashield hard set mounting medium with 4′,6-diamidino-2-phenylindole (DAPI) (Vector) following the manufacturer's directions. Each washing was done for 5 min and all the steps were performed at room temperature unless specified otherwise. For cells that were stained with only phalloidin, the permeabilization step was followed by washing three times with PBS and then incubation with Alexa 488 or ifluor 555 phalloidin in PBS. Images of cells were taken with a 40× objective on a FV1000 confocal microscope (Olympus, Center Valley, PA), processed with Olympus Fluoview Ver.4.2a software, ImageJ, and CorelDRAW X8. Fluorescence intensity was analyzed by Plot Profile in ImageJ software and translocation of RBDRaf1-GFP to the cell cortex was measured as a percent of total cells with cortical RBDRaf1-GFP. Quantification of F-actin, the presence or absence of PakD puncta, and the presence or absence of CnrN localization, were analyzed by blinded observers. In type 354118 eight-well slides (Corning, Big Flat, NY), the front of a cell was defined as the side of the cell facing away from the top right corner, where AprA was added to create an AprA gradient. The back of a cell was defined as the side of the cell facing toward the top right corner. For control wells, where buffer was added to the top right corner, irrespective of the direction of cell movement, the front of a cell was defined as the side of a cell facing away from the top right corner and the back was defined as the side facing toward the top right corner.

Ras activation assay

Ras activity in AX2 wild-type cells was measured using the pull-down assay kit (Cat. #BK008-S; Cytoskeleton, Denver, CO). In brief, 1×10^6

cells/ml were treated with 300 ng/ml rAprA in 20 mM $NaPO_4$ or an equal volume of buffer for 5 min, 5×10^6 cells were collected by centrifugation at 500 × *g* for 3 min and washed once with ice-cold Sørensen buffer (Gerisch *et al.*, 1967), and the pellet was lysed with lysis buffer (provided in the kit). The lysate was clarified by centrifugation at 10,000 × *g* for 1 min at 4°C. Raf-RBD affinity beads were added to the lysate and allowed to bind to the active form of Ras for 1 h at 4°C. Active Ras bound to beads was collected by centrifugation at 5000 × *g* for 1 min at 4°C. Ras bound beads were eluted in 2X SDS sample buffer with protease inhibitors (Thermo Fisher). SDS–PAGE and Coomassie staining of total lysate, and Western blot using anti-pan Ras (provided in the kit) were performed as described below. For quantitation of the immunoblot, bands were normalized to the Ponceau S–stained blot.

Filopod and pseudopod analysis

Filopod and pseudopod projections were analyzed in AprA gradients in an Insall chamber. After using a 10× objective to verify that cells were moving away from the AprA, cells were observed with a 60×/1.4 oil objective on a Nikon Microphot-FX. Images were recorded for 140 s at 2 s intervals. The sizes, locations, frequencies, and lifespans of filopod and pseudopod projections were analyzed in the video images. The Insall chamber has a reservoir A and a reservoir B. Cells on the platform between reservoirs A and B were imaged. If reservoir A had AprA, and B had HL5 medium, the front of a cell was defined as the side of the cell facing reservoir B, and the back was defined as the side of the cell facing reservoir A. For the control, reservoirs A and B both contained HL5, and irrespective of the direction of cell movement, the front was defined as the side of a cell facing toward reservoir B and the back was defined as the side facing reservoir A.

Actin and myosin polymerization, myosin phosphorylation, Akt substrates phosphorylation, and Western blots

Crude cytoskeletons were prepared using a modification of previously described methods (Reines and Clarke, 1985; Dharmawardhane *et al.*, 1989). Cells were grown to 2×10^6 cells/ml in HL5 in shaking culture, collected by centrifugation at 500 × *g* for 3 min, resuspended in HL5, collected by centrifugation, and resuspended to 1×10^7 cells/ml. rAprA (300 ng/ml) in 20 mM $NaPO_4$ or an equal volume of 20 mM $NaPO_4$ was added to 200 µl of cells. For whole cell lysates, at various times after addition, cells were mixed with an equal volume of 2X SDS sample buffer with protease and phosphatase inhibitors (Cell Signaling Technology), heated to 95°C for 3 min, and stored at –70°C. For crude cytoskeletons, at various times after addition, the cells were gently mixed with 1 ml of lysis buffer (100 mM PIPES, pH 6.8, 1 mM $MgCl_2$, 2.5 mM ethylene glycol tetraacetic acid [EGTA], 10 mM TAME [*N*-α-*p*-tosyl-L-arginine methyl ester hydrochloride], 0.5% Triton X-100, and a 50-ml Pierce Protease Inhibitor Tablet, EDTA-free [Thermo Fisher Scientific, Waltham, MA] in each 50 ml of buffer). Samples were kept on ice for 2 min, and cytoskeletons were collected by centrifugation at 15,000 × *g* for 5 min at 4°C. The pellet was resuspended in 0.5 ml of lysis buffer, and cytoskeletons were again collected by centrifugation at 4°C. The pellet was resuspended in 200 µl of 1X SDS sample buffer with protease inhibitors (Thermo Fisher) and heated to 95°C for 3 min and stored at –70°C. Total actin and filamentous actin were detected by electrophoresis of the whole cell lysate and crude cytoskeletons, respectively, on Tris-glycine 4–20% polyacrylamide gels (Lonza, Rockland, ME) and staining with Coomassie Brilliant Blue. Western blots of similar gels were stained for 1 h at room temperature with 1:5000 diluted 3E6cE8 anti-myosin II mouse monoclonal antibody following Suess *et al.* (2017) to detect total myosin II and cytoskeleton-associated myosin II. Myosin phosphorylation was assayed following Tang *et al.* (2002) by staining Western blots of whole cell lysates with 1:1000 42H4 mouse anti-phosphothreonine (Cell Signaling Technology) following the manufacturer's directions. Western blots of whole cell lysates were also stained with 1:1000 rabbit anti-phospho-Akt substrate [RXXS*/T*], anti-phospho-Rac1/Cdc42 [Ser71], or anti-phospho-p44/42 MAPK [ERK1/2] [Thr202/Tyr204] (all from Cell Signaling Technology, following the manufacturer's directions). Bound antibody was detected with ECL Western blotting kits (Thermo Fisher). Band intensities on Western blots were quantified using Image Lab software. For total actin, total myosin, phospho-Akt substrates, phospho-ERK1, and phospho-RacC, for each independent experiment the band intensities were normalized to the band intensity at $t = 0$, and the mean ± SEM for each timepoint from the independent experiments was then calculated. For polymerized actin, for each timepoint in each independent experiment, the polymerized actin band intensity was normalized to the total actin band intensity for that timepoint, and then these values were normalized to the $t = 0$ value. The mean ± SEM of the $t = 0$ normalized values from the independent experiments was then calculated for each timepoint. Polymerized myosin II and phosphorylated myosin II values were calculated as for the polymerized actin.

Statistical analysis

Prism (GraphPad, San Diego, CA) and Microsoft Excel were used for data analysis using *t* tests or analysis of variance (ANOVA) with appropriate posttests. Data are shown as mean ± SEM. Statistical significance was defined as $p < 0.05$.

ACKNOWLEDGMENTS

We thank Robert Insall for kindly providing Insall chambers and *wasA*⁻ cells, Miho Iijima for providing *racC*⁻ cells, Tian Jin for providing *elmoE*⁻ cells, Jane Borleis for providing *plaA*⁻ cells, Wouter–Jan Rappel for providing pDm115RafRBD plasmid, and David Knecht for providing the anti-myosin II antibody. We thank Louis A. Cadena and Merilyn Beebe for performing blinded analysis of the results. The use of the Microscopy and Imaging Center facility at Texas A&M University is acknowledged. The Olympus FV1000 confocal microscope acquisition was supported by the Office of the Vice President for Research at Texas A&M University. We thank two anonymous reviewers for helping to improve the clarity of the manuscript. This work was supported by National Institutes of Health Grant no. GM-118355.

REFERENCES

Affolter M, Weijer CJ (2005). Signaling to cytoskeletal dynamics during chemotaxis. Dev Cell 9, 19–34.

Andrew N, Insall RH (2007). Chemotaxis in shallow gradients mediated independently of PtdIns 3-kinase by biased choices between random protrusions. Nat Cell Biol 9, 193–200.

Bakthavatsalam D, Choe JM, Hanson NE, Gomer RH (2009). A *Dictyostelium* chalone uses G proteins to regulate proliferation. BMC Biol 7, 44.

Berlot CH, Spudich JA, Devreotes PN (1985). Chemoattractant-elicited increases in myosin phosphorylation in *Dictyostelium*. Cell 43, 307–314.

Blagg SL, Stewart M, Sambles C, Insall RH (2003). PIR121 regulates pseudopod dynamics and SCAR activity in *Dictyostelium*. Curr Biol 13, 1480–1487.

Bloomfield G, Traynor D, Sander SP, Veltman DM, Pachebat JA, Kay RR (2015). Neurofibromin controls macropinocytosis and phagocytosis in *Dictyostelium*. eLife 4, e04940.

Bolourani P, Spiegelman GB, Weeks G (2006). Delineation of the roles played by RasG and RasC in cAMP-dependent signal transduction

during the early development of *Dictyostelium discoideum*. Mol Biol Cell 17, 4543–4550.
Bosgraaf L, van Haastert PJ (2009). Navigation of chemotactic cells by parallel signaling to pseudopod persistence and orientation. PLoS One 4, e6842.
Brock DA, Gomer RH (1999). A cell-counting factor regulating structure size in *Dictyostelium*. Genes Dev 13, 1960–1969.
Brock DA, Gomer RH (2005). A secreted factor represses cell proliferation in *Dictyostelium*. Development 132, 4553–4562.
Cai H, Das S, Kamimura Y, Long Y, Parent CA, Devreotes PN (2010). Ras-mediated activation of the TORC2-PKB pathway is critical for chemotaxis. J Cell Biol 190, 233–245.
Cargnello M, Roux PP (2011). Activation and function of the MAPKs and their substrates, the MAPK-activated protein kinases. Microbiol Mol Biol Rev 75, 50–83.
Chen L, Iijima M, Tang M, Landree MA, Huang YE, Xiong Y, Iglesias PA, Devreotes PN (2007). PLA2 and PI3K/PTEN pathways act in parallel to mediate chemotaxis. Dev Cell 12, 603–614.
Choe JM, Bakthavatsalam D, Phillips JE, Gomer RH (2009). *Dictyostelium* cells bind a secreted autocrine factor that represses cell proliferation. BMC Biochem 10, 4.
Comer FI, Lippincott CK, Masbad JJ, Parent CA (2005). The PI3K-mediated activation of CRAC independently regulates adenylyl cyclase activation and chemotaxis. Curr Biol 15, 134–139.
Comer FI, Parent CA (2002). PI 3-kinases and PTEN. Cell 109, 541–544.
Cramer LP, Kay RR, Zatulovskiy E (2018). Repellent and attractant guidance cues initiate cell migration by distinct rear-driven and front-driven cytoskeletal mechanisms. Curr Biol 28, 995–1004.e3.
Davidson AJ, Amato C, Thomason PA, Insall RH (2018). WASP family proteins and formins compete in pseudopod- and bleb-based migration. J Cell Biol 217, 701–714.
de Oliveira S, Rosowski EE, Huttenlocher A (2016). Neutrophil migration in infection and wound repair: going forward in reverse. Nat Rev Immunol 16, 378–391.
Dembinsky A, Rubin H, Ravid S (1997). Autophosphorylation of *Dictyostelium* myosin II heavy chain-specific protein kinase C is required for its activation and membrane dissociation. J Biol Chem 272, 828–834.
Devreotes P, Horwitz AR (2015). Signaling networks that regulate cell migration. Cold Spring Harb Perspect Biol 7, a005959.
de Wit RJ, Bulgakov R (1985). Guanine nucleotides modulate the ligand binding properties of cell surface folate receptors in *Dictyostelium discoideum*. FEBS Lett 179, 257–261.
Dharmawardhane S, Warren V, Hall AL, Condeelis J (1989). Changes in the association of actin-binding proteins with the actin cytoskeleton during chemotactic stimulation of *Dictyostelium discoideum*. Cell Motil Cytoskeleton 13, 57–63.
Eden S, Rohatgi R, Podtelejnikov AV, Mann M, Kirschner MW (2002). Mechanism of regulation of WAVE1-induced actin nucleation by Rac1 and Nck. Nature 418, 790–793.
Fey P, Dodson RJ, Basu S, Chisholm RL (2013). One stop shop for everything *Dictyostelium*: dictyBase and the Dicty Stock Center in 2012. Methods Mol Biol 983, 59–92.
Garcia M, Ray S, Brown I, Irom J, Brazill D (2014). PakD, a putative p21-activated protein kinase in *Dictyostelium discoideum*, regulates actin. Eukaryot Cell 13, 119–126.
Gerisch G, Luderitz O, Ruschmann E (1967). Antibodies promoting phagocytosis of bacteria by amoebae. Z Naturforsch B 22, 109.
Hadwiger JA, Lee S, Firtel RA (1994). The G alpha subunit G alpha 4 couples to pterin receptors and identifies a signaling pathway that is essential for multicellular development in *Dictyostelium*. Proc Natl Acad Sci USA 91, 10566–10570.
Hadwiger JA, Nguyen HN (2011). MAPKs in development: insights from *Dictyostelium* signaling pathways. Biomol Concepts 2, 39–46.
Han JW, Leeper L, Rivero F, Chung CY (2006). Role of RacC for the regulation of WASP and phosphatidylinositol 3-kinase during chemotaxis of *Dictyostelium*. J Biol Chem 281, 35224–35234.
Heid PJ, Geiger J, Wessels D, Voss E, Soll DR (2005). Computer-assisted analysis of filopod formation and the role of myosin II heavy chain phosphorylation in *Dictyostelium*. J Cell Sci 118, 2225–2237.
Herlihy SE, Brown ML, Pilling D, Weeks BR, Myers LK, Gomer RH (2015). Role of the neutrophil chemorepellent soluble dipeptidyl peptidase IV in decreasing inflammation in a murine model of arthritis. Arthritis Rheumatol 67, 2634–2638.
Herlihy SE, Pilling D, Maharjan AS, Gomer RH (2013a). Dipeptidyl peptidase IV is a human and murine neutrophil chemorepellent. J Immunol 190, 6468–4677.
Herlihy SE, Tang Y, Gomer RH (2013b). A *Dictyostelium* secreted factor requires a PTEN-like phosphatase to slow proliferation and induce chemorepulsion. PLoS One 8, e59365.
Herlihy SE, Tang Y, Phillips JE, Gomer RH (2017). Functional similarities between the dictyostelium protein AprA and the human protein dipeptidyl-peptidase IV. Protein Sci 26, 578–585.
Ibarra N, Blagg SL, Vazquez F, Insall RH (2006). Nap1 regulates *Dictyostelium* cell motility and adhesion through SCAR-dependent and -independent pathways. Curr Biol 16, 717–722.
Iijima M, Devreotes P (2002). Tumor suppressor PTEN mediates sensing of chemoattractant gradients. Cell 109, 599–610.
Kamimura Y, Xiong Y, Iglesias PA, Hoeller O, Bolourani P, Devreotes PN (2008). PIP3-independent activation of TorC2 and PKB at the cell's leading edge mediates chemotaxis. Curr Biol 18, 1034–1043.
Keizer-Gunnink I, Kortholt A, van Haastert PJ (2007). Chemoattractants and chemorepellents act by inducing opposite polarity in phospholipase C and PI3-kinase signaling. J Cell Biol 177, 579–585.
Klein PS, Sun TJ, Saxe CL 3rd, Kimmel AR, Johnson RL, Devreotes PN (1988). A chemoattractant receptor controls development in *Dictyosteliumdiscoideum*. Science 241, 1467–1472.
Knecht DA, Loomis WF (1987). Antisense RNA inactivation of myosin heavy chain gene expression in *Dictyostelium discoideum*. Science 236, 1081–1086.
Kolaczkowska E, Kubes P (2013). Neutrophil recruitment and function in health and inflammation. Nat Rev Immunol 13, 159–175.
Kortholt A, Kataria R, Keizer-Gunnink I, van Egmond WN, Khanna A, van Haastert PJ (2011). *Dictyostelium* chemotaxis: essential Ras activation and accessory signalling pathways for amplification. EMBO Rep 12, 1273–1279.
Kortholt A, van Haastert PJ (2008). Highlighting the role of Ras and Rap during *Dictyostelium* chemotaxis. Cell Signal 20, 1415–1422.
Kumagai A, Pupillo M, Gundersen R, Miake-Lye R, Devreotes PN, Firtel RA (1989). Regulation and function of Gαprotein subunits in *Dictyostelium*. Cell 57, 265–275.
Lee S, Comer FI, Sasaki A, Mcleod IX, Duong Y, Okumura K, Yates JR, 3RD, Parent CA, Firtel RA (2005). TOR complex 2 integrates cell movement during chemotaxis and signal relay in *Dictyostelium*. Mol Biol Cell 16, 4572–4583.
Levi S, Polyakov MV, Egelhoff TT (2002). Myosin II dynamics in *Dictyostelium*: determinants for filament assembly and translocation to the cell cortex during chemoattractant responses. Cell Motil Cytoskeleton 53, 177–188.
Liang W, Warrick HM, Spudich JA (1999). A structural model for phosphorylation control of *Dictyostelium* myosin II thick filament assembly. J Cell Biol 147, 1039–1048.
Lilly PJ, Devreotes PN (1995). Chemoattractant and GTP gamma S-mediated stimulation of adenylyl cyclase in *Dictyostelium* requires translocation of CRAC to membranes. J Cell Biol 129, 1659–1665.
Lilly P, Wu L, Welker DL, Devreotes PN (1993). A G-protein beta-subunit is essential for *Dictyostelium* development. Genes Dev 7, 986–995.
Lim CJ, Spiegelman GB, Weeks G (2001). RasC is required for optimal activation of adenylyl cyclase and Akt/PKB during aggregation. EMBO J 20, 4490–4499.
Lim CJ, Zawadzki KA, Khosla M, Secko DM, Spiegelman GB, Weeks G (2005). Loss of the *Dictyostelium* RasC protein alters vegetative cell size, motility and endocytosis. Exp Cell Res 306, 47–55.
Lusche DF, Wessels D, Scherer A, Daniels K, Kuhl S, Soll DR (2012). The IplA Ca^{2+} channel of *Dictyostelium discoideum* is necessary for chemotaxis mediated through Ca^{2+}, but not through cAMP, and has a fundamental role in natural aggregation. J Cell Sci 125, 1770–1783.
Ma H, Gamper M, Parent C, Firtel RA (1997). The *Dictyostelium* MAP kinase kinase DdMEK1 regulates chemotaxis and is essential for chemoattractant-mediated activation of guanylyl cyclase. EMBO J 16, 4317–4332.
Maehama T, Dixon JE (1998). The tumor suppressor, PTEN/MMAC1, dephosphorylates the lipid second messenger, phosphatidylinositol 3,4,5-trisphosphate. J Biol Chem 273, 13375–13378.
Mann SK, Firtel RA (1991). A developmentally regulated, putative serine/threonine protein kinase is essential for development in *Dictyostelium*. Mech Dev 35, 89–101.
Meili R, Ellsworth C, Firtel RA (2000). A novel Akt/PKB-related kinase is essential for morphogenesis in *Dictyostelium*. Curr Biol, 10, 708–717.
Mohamed W, Ray S, Brazill D, Baskar R (2015). Absence of catalytic domain in a putative protein kinase C (PkcA) suppresses tip dominance in *Dictyostelium discoideum*. Dev Biol 405, 10–20.

Muinonen-Martin AJ, Veltman DM, Kalna G, Insall RH (2010). An improved chamber for direct visualisation of chemotaxis. PLoS One 5, e15309.
Myers SA, Han JW, Lee Y, Firtel RA, Chung CY (2005). A *Dictyostelium* homologue of WASP is required for polarized F-actin assembly during chemotaxis. Mol Biol Cell 16, 2191–2206.
Nguyen HN, Raisley B, Hadwiger JA (2010). MAP kinases have different functions in *Dictyostelium* G protein-mediated signaling. Cell Signal 22, 836–847.
Nichols JM, Veltman D, Kay RR (2015). Chemotaxis of a model organism: progress with *Dictyostelium*. Curr Opin Cell Biol 36, 7–12.
Nourshargh S, Renshaw SA, Imhof BA (2016). Reverse migration of neutrophils: where, when, how, and why? Trends Immunol 37, 273–286.
Para A, Krischke M, Merlot S, Shen Z, Oberholzer M, Lee S, Briggs S, Firtel RA (2009). *Dictyostelium* Dock180-related RacGEFs regulate the actin cytoskeleton during cell motility. Mol Biol Cell 20, 699–707.
Parent CA, Devreotes PN (1996). Molecular genetics of signal transduction in *Dictyostelium*. Annu Rev Biochem 65, 411–440.
Peracino B, Borleis J, Jin T, Westphal M, Schwartz JM, Wu L, Bracco E, Gerisch G, Devreotes P, Bozzaro S (1998). G protein β subunit–null mutants are impaired in phagocytosis and chemotaxis due to inappropriate regulation of the actin cytoskeleton. J Cell Biol 141, 1529–1537.
Phillips JE, Gomer RH (2012). A secreted protein is an endogenous chemorepellant in *Dictyostelium discoideum*. Proc Natl Acad Sci USA 109, 10990–10995.
Phillips JE, Gomer RH (2014). The p21-activated kinase (PAK) family member PakD is required for chemorepulsion and proliferation inhibition by autocrine signals in *Dictyostelium discoideum*. PLoS One 9, e96633.
Ravid S, Spudich JA (1989). Myosin heavy chain kinase from developed *Dictyostelium* cells. Purification and characterization. J Biol Chem 264, 15144–15150.
Reines D, Clarke M (1985). Immunochemical analysis of the supramolecular structure of myosin in contractile cytoskeletons of *Dictyostelium* amoebae. J Biol Chem 260, 14248–14254.
Roelofs J, Snippe H, Kleineidam RG, van Haastert PJ (2001). Guanylate cyclase in *Dictyostelium discoideum* with the topology of mammalian adenylate cyclase. Biochem J 354, 697–706.
Roelofs J, van Haastert PJ (2002). Characterization of two unusual guanylyl cyclases from *Dictyostelium*. J Biol Chem 277, 9167–9174.
Sadik CD, Luster AD (2012). Lipid-cytokine-chemokine cascades orchestrate leukocyte recruitment in inflammation. J Leukoc Biol 91, 207–215.
Santorelli LA, Thompson CR, Villegas E, Svetz J, Dinh C, Parikh A, Sucgang R, Kuspa A, Strassmann JE, Queller DC, Shaulsky G (2008). Facultative cheater mutants reveal the genetic complexity of cooperation in social amoebae. Nature 451, 1107–1110.
Sasaki AT, Chun C, Takeda K, Firtel RA (2004). Localized Ras signaling at the leading edge regulates PI3K, cell polarity, and directional cell movement. J Cell Biol 167, 505–518.
Scavello M, Petlick AR, Ramesh R, Thompson VF, Lotfi P, Charest PG (2017). Protein kinase A regulates the Ras, Rap1, and TORC2 pathways in response to the chemoattractant cAMP in *Dictyostelium*. J Cell Sci 130, 1545–1558.
Schmidt A, Kunz J, Hall MN (1996). TOR2 is required for organization of the actin cytoskeleton in yeast. Proc Natl Acad Sci USA, 93, 13780–13785.
Schwarz J, Proff J, Havemeier A, Ladwein M, Rottner K, Barlag B, Pich A, Tatge H, Just I, Gerhard R (2012). Serine-71 phosphorylation of Rac1 modulates downstream signaling. PLoS One 7, e44358.
Schwebs DJ, Hadwiger JA (2015). The *Dictyostelium* MAPK ERK1 is phosphorylated in a secondary response to early developmental signaling. Cell Signal 27, 147–155.
Shaulsky G, Escalante R, Loomis WF (1996). Developmental signal transduction pathways uncovered by genetic suppressors. Proc Natl Acad Sci USA 93, 15260–15265.
Sobko A, Ma H, Firtel RA (2002). Regulated SUMOylation and ubiquitination of DdMEK1 is required for proper chemotaxis. Dev Cell 2, 745–756.
Suess PM, Watson J, Chen W, Gomer RH (2017). Extracellular polyphosphate signals through Ras and Akt to prime *Dictyostelium discoideum* cells for development. J Cell Sci 130, 2394–2404.
Sun HY, King AJ, Diaz HB, Marshall MS (2000). Regulation of the protein kinase Raf-1 by oncogenic Ras through phosphatidylinositol 3-kinase, Cdc42/Rac and Pak. Curr Biol 10, 281–284.
Tang L, Gao T, Mccollum C, Jang W, Vicker MG, Ammann RR, Gomer RH (2002). A cell number-counting factor regulates the cytoskeleton and cell motility in *Dictyostelium*. Proc Natl Acad Sci USA 99, 1371–1376.
Tang Y, Gomer RH (2008). A protein with similarity to PTEN regulates aggregation territory size by decreasing cyclic AMP pulse size during *Dictyostelium discoideum* development. Eukaryot Cell 7, 1758–1770.
Tang M, Iijima M, Kamimura Y, Chen L, Long Y, Devreotes P (2011). Disruption of PKB signaling restores polarity to cells lacking tumor suppressor PTEN. Mol Biol Cell 22, 437–447.
Tang Y, Wu Y, Herlihy SE, Brito-Aleman FJ, Ting JH, Janetopoulos C, Gomer RH (2018). An autocrine proliferation repressor regulates *Dictyostelium discoideum* proliferation and chemorepulsion using the G protein-coupled receptor GrlH. MBio 9.
Tang Y, Yu J, Field J (1999). Signals from the Ras, Rac, and Rho GTPases converge on the Pak protein kinase in Rat-1 fibroblasts. Mol Cell Biol 19, 1881–1891.
Theveneau E, Mayor R (2012). Neural crest delamination and migration: from epithelium-to-mesenchyme transition to collective cell migration. Dev Biol 366, 34–54.
Traynor D, Milne JL, Insall RH, Kay RR (2000). Ca^{2+} signalling is not required for chemotaxis in *Dictyostelium*. EMBO J 19, 4846–4854.
van Haastert PJ, van Driel R, Jastorff B, Baraniak J, Stec WJ, de Wit RJ (1984). Competitive cAMP antagonists for cAMP-receptor proteins. J Biol Chem 259, 10020–10024.
van Haastert PJM (2010). Chemotaxis: insights from the extending pseudopod. J Cell Sci 123, 3031–3037.
van Haastert PJM, Kuwayama H (1997). cGMP as second messenger during *Dictyostelium* chemotaxis. FEBS Lett 410, 25–28.
Veltman DM, King JS, Machesky LM, Insall RH (2012). SCAR knockouts in Dictyostelium: WASP assumes SCAR's position and upstream regulators in pseudopods. J Cell Biol 198, 501–508.
Veltman DM, Lemieux MG, Knecht DA, Insall RH (2014). PIP(3)-dependent macropinocytosis is incompatible with chemotaxis. J Cell Biol 204, 497–505.
Wang Y, Senoo H, Sesaki H, Iijima M (2013). Rho GTPases orient directional sensing in chemotaxis. Proc Natl Acad Sci USA 110, E4723–E4732.
Wessels D, Lusche DF, Kuhl S, Heid P, Soll DR (2007). PTEN plays a role in the suppression of lateral pseudopod formation during *Dictyostelium* motility and chemotaxis. J Cell Sci 120, 2517–2531.
White MJV, Chinea LE, Pilling D, Gomer RH (2018). Protease activated-receptor 2 is necessary for neutrophil chemorepulsion induced by trypsin, tryptase, or dipeptidyl peptidase IV. J Leukoc Biol 103, 119–128.
White MJ, Galvis-Carvajal E, Gomer RH (2015). A brief exposure to tryptase or thrombin potentiates fibrocyte differentiation in the presence of serum or serum amyloid p. J Immunol 194, 142–150.
Wu L, Gaskins C, Zhou K, Firtel RA, Devreotes PN (1994). Cloning and targeted mutations of Gα7 and Gα8, two developmentally regulated G protein α-subunit genes in *Dictyostelium*. Mol Biol Cell 5, 691–702.
Wu LJ, Valkema R, Van Haastert PJM, Devreotes PN (1995). The G protein β subunit is essential for multiple responses to chemoattractants in *Dictyostelium*. J Cell Biol 129, 1667–1675.
Yan J, Mihaylov V, Xu X, Brzostowski JA, Li H, Liu L, Veenstra TD, Parent CA, Jin T (2012). A Gβγ effector, ElmoE, transduces GPCR signaling to the actin network during chemotaxis. Dev Cell 22, 92–103.
Yuen IS, Gomer RH (1994). Cell density-sensing in *Dictyostelium* by means of the accumulation rate, diffusion coefficient and activity threshold of a protein secreted by starved cells. J Theor Biol 167, 273–282.
Zaki M, Andrew N, Insall RH (2006). *Entamoeba histolytica* cell movement: a central role for self-generated chemokines and chemorepellents. Proc Natl Acad Sci USA 103, 18751–18756.
Zoncu R, Efeyan A, Sabatini DM (2011). mTOR: from growth signal integration to cancer, diabetes and ageing. Nat Rev Mol Cell Biol 12, 21–35.